Chapter 2
Engineering Deformation Compatibility Control Method and Structural Safety Management

Engineering structure-related stable equilibrium and deformation compatibility control method is an effective technique for ensuring the safety of engineering structures. Engineering structure designs improve stress analysis to an analysis that considers both stress and deformation of engineering structure. Thus, the stable equilibrium and DCC of engineering structures can be achieved, thereby preventing latent risks in some engineering structures that are designed based on the concept of equilibrium and failure. Engineering structure-related stable equilibrium and deformation compatibility control method is similar to A × a. Stable equilibrium refers to that A is the stable equilibrium problem examined in the application of classical Newtonian mechanics or contemporary engineering mechanics; and DCC refers to that a is often neglected and incomplete in relevant discourses. In actuality, A × a exhibits a coupling relationship. DCC of engineering structures involves two aspects: (1) Structure stability and load and deformation compatibility render engineering structures in design or normal stress–deformation state. In other words, the actual path of force transmission and designed path of force transmission in the structure are similar or identical. (2) Weak parts or vulnerable parts of an engineering structure must be controlled in advance to prevent damage concentration. Therefore, DCC of engineering structures is the prerequisite for examining problems of stable equilibrium in these structures by using classical Newtonian mechanics or contemporary engineering mechanics. DCC problems of an engineering structure should be determined from a macroscopic perspective of physics of engineering structures. Correct conclusion can therefore be drawn from the use of classical Newtonian mechanics or contemporary engineering mechanics in examining stable equilibrium problems in engineering structures. Consequently, stable equilibrium and DCC of engineering structures can be achieved to ensure the safety of these structures.

© Shanghai Jiao Tong University Press, Shanghai and Springer Science+Business Media Singapore 2017

H. Zhu et al., *Deformation Compatibility Control for Engineering Structures*,
DOI 10.1007/978-981-10-1893-0_2

2.1 Effect of Deformation Compatibility Control on the Transmission or Transfer of Force in Structural Systems

Conversion of external work into elastic strain energy or other forms of energy is a natural physical phenomenon in engineering structures. To effectively and steadily convert the external work of an equilibrium system into elastic strain energy, sufficient energy must be available for spatial or path conversion (i.e., DCC) so that the structure can withstand external force through deformation. Subsequently, force transmission and energy conversion are performed according to the designed path, thus achieving stable equilibrium.

Specifically, DCC requires the structure to possess adequate space for deformation and appropriate rigidity matching. Structures with excessive rigidity exhibit poor deformation capability; if displacement difference is generated, then the structure must bear a substantial external load, which easily causes localized damage and eventually leads to complete destruction. Although structures with overly low rigidity can effectively eliminate external force, it easily induces excessively large deformation, rendering the structure nonfunctional, which may even cause overturning of the entire structure. Several composite systems made of different structures are often problematic because DCC-related problems are improperly handled. For example, double-curved arch bridge, rigid-framed arch bridge, and mortar stone arch bridge constructed in the 1960s–1980s, as well as new bridges made recently of different combinations of bridge structures cannot be converted from combined or single load-bearing body to a load-bearing body as a whole. Restrictors installed between the cables of large-span cable stayed bridge and between high-voltage cables facilitate such cables to function as designed. Filling foams or foam concrete in the space where landslide occurs near road tunnels can provide a buffer space for mitigating the effect of localized landslide. In essence, this process reduces the effect of external work and effectively converts it into elastic strain energy that provides sufficient energy for spatial or path conversion. This shows that the layout of a structure and structural measures that are based on DCC concept can be employed to ensure the accuracy of calculation assumptions and stress analysis, thereby controlling the behavior of the structure.

Analysis of structural mechanics can be conducted to examine the mechanical behavior and process of the research base and structural composite system. Effective measures can be adopted, if necessary, to ensure that the entire engineering structure construction process meets the conditions of the research base and structural system. Thus, stable equilibrium and DCC can be maintained, and external work can be converted into elastic strain energy. Consequently, a composite structural system that bears load independently can be transformed from a combined or single load-bearing body to a load-bearing body that bears load as a whole. Otherwise, the initial form of equilibrium can be changed into a new form of equilibrium, and this novel form of equilibrium may exhibit unfavorable stability. Concerning composite structural systems that contain multiple independent

load-bearing units, which cannot achieve DCC, cracks in the connection areas of these systems must be avoided. For instance, the load-bearing independency of double-arched tunnels, tunnels with small interval, and multiple, independent, parallel continuous skew bridges must be enhanced.

Structural mechanics, energy methods, and other related theories can solve structure stable equilibrium problems. Hooke's Law and constitutive relations theories provide the relationship between stressed materials and deformation. Structure DCC problems do not manifest problems concerning effective force transmission inside components or between components and a clear analytical standard for them is also lacking. For complex structures, engineering methods and structural innovation have solved majority of connection reliability problems; however, ascertaining whether the connection between components and inside nonuniform components satisfies DCC conditions is difficult and it might not satisfy such conditions. Previous studies have not paid adequate attention to this problem, which sometimes causes cracks in the structure, negatively affects deformation, and leads to structural failure.

When a structure is incompatible to deformation, the structure is in equilibrium but it is in different states. In complex structures (particularly flexible ones), path of force transmission changes or additional internal force which may even exceed the internal force of load can be produced. Subsequently, the structure likely forms cracks or fails, thereby entering a state of unstable equilibrium. Alternatively, the load-bearing approach of the structural system may be affected, which changes the path of force transmission or transfer. Thus, undesired stress concentration or unwanted changes in load-bearing mechanisms (changes in tension and compression) may occur in certain parts of the structure, disrupting the original or designed stable equilibrium state in the structural system and forming a new design equilibrium state that has not been examined before. These risk factors may within the safety limit of the structures, pose risks or induce cracks in the structure, or render structural construction or operational risks uncontrollable, thereby jeopardizing the safety of the structures.

Therefore, design and construction of engineering structures should focus on target control, that is, the equilibrium state $\Sigma P_i = 0$ on completion of the construction of the structure. In fact, when deformation incompatibility occurs during the construction or use of the structure, force and energy are redistributed or transferred. If process control is neglected in design and construction processes, it may affect the factors or conditions of the original equilibrium equation $\Sigma P_i = 0$. Thus, the initial equilibrium states are likely changed or disrupted, causing $\Sigma P_i \neq 0$. Hence, the design and construction processes must comprehensively consider the mutual relationships between the four factors of system detail, equilibrium stability, target control, and process control. Thus, construction skills, suitable engineering structures and their material properties, as well as environmental conditions can be integrated to achieve collective stress bearing and DCC and prevent the degeneration of weak parts.

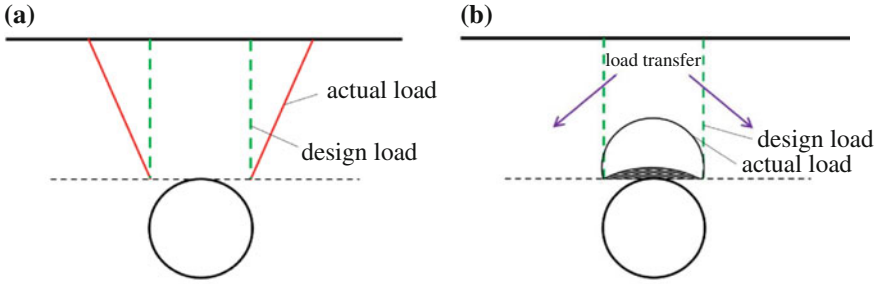


Fig. 2.1 Schematic diagram illustrating the bearing of load by deep-embedded culvert. **a** Culvert load exhibiting inverted trapezoidal-like distribution. **b** Culvert load exhibiting collapsing-like distribution

Example 2.1.1 Load-bearing analysis of deep-embedded culvert describes the effects of DCC on the transmission or transfer of force in a structural system. To date, numerous problems associated with embedded culvert cracks have been identified. According to an analysis of Fig. 2.1a, because the culvert rigidity is greater than subgrade rigidity, design culvert load, which exhibits uniform distribution, is smaller than the actual culvert load, which exhibits inverted trapezoidal-like distribution. The excess load on shallow-embedded culvert is within the safety limit. Excess load on deep-embedded culvert may cause culvert crack, which is in fact the weakness of deep-embedded culverts. Thus, transferring unfavorable force and energy to culvert structures or concentrating them on such structures should be avoided.

According to Fig. 2.1b, because the culvert is coated with lightweight material, the rigidity of such composite system (culvert and lightweight material) is smaller than the subgrade rigidity. The design culvert load, which exhibits uniform distribution, is greater than the actual culvert load, which exhibits collapsing-like distribution. The load from the top is transferred to the subgrade; this way, the load on shallow-embedded and deep-embedded culverts is kept within the safety limit, protecting the culvert from cracking.

Example 2.1.2 As statistics show, the types of bridges and beams that were involved in accidents in recent years include simple support beams, composite arch bridge, and rigid frame bridge, all of which are classified as flexible structures or a combination of flexible and rigid structures. Because these types of structures are often in a state of elastoplasticity and are subjected to high cyclic stress or unfavorable stress effects, the load-bearing process of these structures does not exhibit superposition property, the load-bearing state of the structures and loading are path-dependent (equivalent to State 2). Furthermore, vehicles have variable repeated loading path, unlike trains or industrial cranes that have relatively stable

repeated vertical loading path. Thus, flexible structures and composite flexible and rigid structures may generate a substantial difference between design stress and actual stress in bridges under repeated automobile loading path with a portion of excessive load. Meanwhile, elastoplastic structures are prone to accumulated damage compared with flexible structures; thus, unfavorable force and energy are transferred to or concentrated on the weak parts of elastoplastic structures, thereby reducing the lifespan of bridges. Reduced lifespan may cause early bridge failure or cyclical failure, posing safety risks to drivers on the road. Design regulations for train or industrial crane load state that flexible structures shall have identical design stress and actual stress to minimize driving risks (equivalent to State 1). For example, a standard 20-m beam has a weight of 26 t and vehicle has a maximum regulated mass of 55 t; each beam can withstand approximately 27.5 t of mass. In particular, under overload, the structure is often in an elastoplasticity state, rendering it prone to accumulated damage, which incurs greater driving risk (equivalent to State 2). A well-known structural engineer, Mao Yisheng, took part in designing and constructing Qiantang River Bridge, which is a mature steel truss bridge. The bridge is characterized by rigidity, high degree of safety, stable material weight, and flexibility. These characteristics enable structures to sustain minimal accumulated damage and ensure driving safety (equivalent to State 1).

2.2 Application Effectiveness of Deformation Compatibility Control Method in Bridge Structures

Under repeated overload, previous highway small span bridges and some special bridge components exhibit accelerated damage accumulation on nonelastic parts. Particularly, optimized bridges in the 1980s are largely problematic. Previous design methods cannot avoid the aforementioned problems; thus, overload easily causes highway bridge collapse. The core problem is the **difficulty to protect the compatibility of structure force transmission medium while avoiding structure metastable equilibrium**.

The key to applying the DCC method is ensuring that bridge structures transmit force along the designed path. Inadequate force control negatively affects force transfer. Improving designs according to DCC method would adequately increase the rigidity of highway small span bridges and improve DC of some special bridge components. Under repeated overload, nonelastic parts of the bridge that sustain accumulated damage can be controlled to avoid overload-induced bridge collapse. Subsequently, **suitability of structure force transmission medium is protected and structure metastable equilibrium is prevented. Thus, safety of engineering structures is ensured**.

2.2.1 Comparison of Damage Accumulation on Simple Support Bridge Before and After Bridge Reinforcement

For bridge structure under repeated load, as long as the stress exerted falls below the material fatigue limit, cyclic load barely damages the structure. However, under conditions of high stress, stress concentration, large deformed component, and combination of deformation incompatible components, a structure is not entirely elastic. In addition to external work being converted into elastic strain energy, other forms of energy are generated (e.g., thermal energy emitted from fracture opening of fractured column). Then, fatigue induces damage accumulation on the structure, which is also simultaneously a form of energy consumption that influences the lifespan of the structure. For example, assuming a 20-m bridge structure has a fissure reinforced concrete beam with low rigidity; a portion of the surface of a half-through reinforced concrete ribbed arch bridge is a floating system, in which the short boom bears not only tensile force (included in calculation) but also bending shear force (excluded from calculation), and long–short booms deform in different manners, which causes nonuniform bearing of load; and an arch bridge structure has inadequate measure for prevention of boom corrosion. All of these structures are prone to fatigue and damage accumulation. Therefore, merely using static force analysis is inadequate for explaining why most mid-to-small span bridges collapse suddenly under heavy traffic load. Therefore, accumulated fatigue theory and the "principle of energy consumption minimization" must be integrated to analyze these types of structures. In fact, only ideal flexible bodies exhibit external work that is equal to their strain energy, whereas nonelastic bodies generate elastic strain energy in addition to energy that incurs accumulated damage on the structure, causing material deterioration (Fig. 2.2).

For structures designed according to construction and transportation regulations, a structure is considered to be working until that structure enters an elastoplastic state. Although structures are in state of flexibility when under normal use, trunk

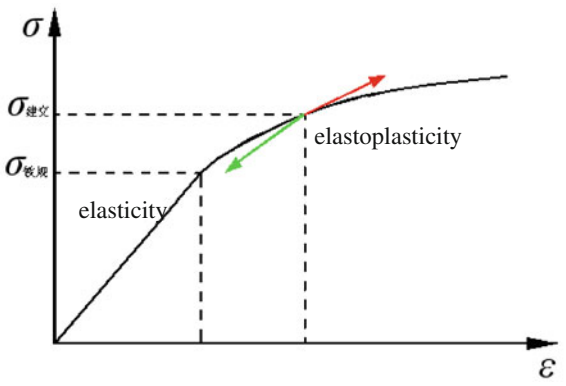


Fig. 2.2 Comparison of damage accumulation on nonelastic bodies under static and repeated loads

highway bridges in fact often withstand heavy loads and even overloads during large traffic volume. Such repeated loads easily result in damage accumulation. Structures designed according to railroad regulations are allowed to work only in a state of elasticity. Railroads generally do not sustain overloads; therefore, railroads rarely sustain accumulated damage when subjected to repeated load (Fig. 2.2). In addition, construction regulations mandate that when calculating the bending capacity of steel bridges that do not directly bear dynamic load (modified to fatigue calculation later on), the calculation can take into consideration that the cross sections enter plasticity state. In other words, the design is made according to elastoplasticity theory. When the bridge directly sustains dynamic load, specifications regulate that bending capacity calculation can be conducted only according to elastic theory. Accordingly, the International Organization for Standardization devised two regulations: (1) Plastic structure design cannot be applied to components exhibiting alternating plasticity. In other words, tension-based yield and compression-based yield are forbidden. (2) Structure bearing dynamic loads cannot have a design load exceeding shakedown load. In other words, component failure shall not occur due to gradual accumulation of plastic deformation; it shall also not cause low cyclic fatigue and failure in materials caused by alternating tension-based and compression-based yields. Occasional incidents of trunk highway bridge collapse, as opposed to railroad bridge collapse, occur around the world. On the same segment of highway, only a few types of bridge collapse after a period of operation. All of these bridges are under a similar state of overload. This phenomenon is similar to the breaking of steel wires in daily life. After just a few cycles of bending, a wire breaks because several cycles of bending activate a state of elastoplasticity in the wire, which causes unfavorable force and energy to be transferred to or concentrated on the weak parts of the wire. The aforementioned two scenarios highlight the importance of elastic working state in trunk highway bridge structures.

When a structure is incompatible to deformation, the load-bearing ability and energy conversion of such structure cannot be performed following the design transmission or transfer path. This type of structure may be in metastable equilibrium or unstable equilibrium (States 2 and 3). If external force or external work is small and the structure demonstrates deformation compatibility, then the structure is in stable equilibrium (State 1). However, the structure experiences fatigue under repeated load and subsequently sustain accumulated damage. Accumulation of damage influences structure lifespan and eventually leads to structural failure, just as how people die from overexertion because long-term intense labor affects people's health and life span.

Regarding damage accumulation in structures, although the deformation and load bearing of structures in practice do not cause structural mutation, the effects of accumulated damage under repeated load expose trunk highway bridges to risks of mutation when under load or deformation because of frequent heavy traffic volume and traffic overload. Load-bearing or deforming structures gradually transition to a state of metastable equilibrium or even to a state of unstable equilibrium. Ultimately, structure failure occurs. Thus, prevention of structure failure should be strengthened. This is particularly crucial for structures with poor material property

and those that experience large traffic flow, partial overload, and nonuniform distribution of load, which are conditions that may exacerbate DCC problems and intensify accumulated damage on these structures.

Example 2.2.1 Failure test was conducted on a 20-m hollow slab beam structure of a certain railway overpass bridge in China. Figure 2.3 is a schematic diagram illustrating a hollow slab beam bearing load. Stage loading approach was used to pass load through a dowel joint to a slab beam to simulate vehicle load. Once the slab beam deformed and stabilized, the deflection of the midspan was recorded and the breadth of the crack on the bottom of the midspan was measured. After unloading, the width of the crack was measured again. Tests were conducted on two types of cross-section hollow slab beams (Slab Beams No. 3 and No. 5 as shown in Fig. 2.4). For Slab Beam No. 3, deflection changes and crack were recorded simultaneously, whereas only the changes in crack were recorded for Slab Beam No. 5.

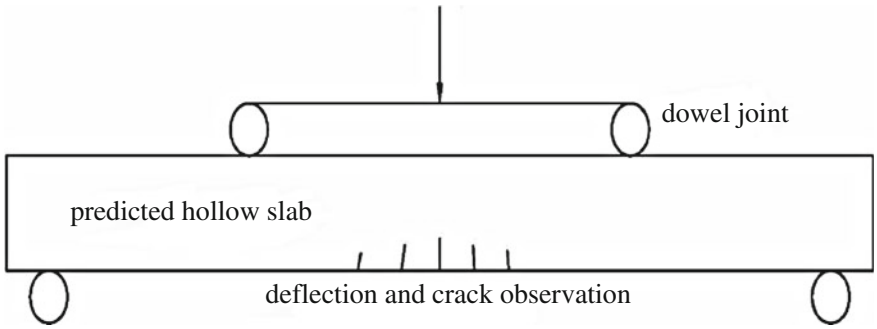


Fig. 2.3 Schematic diagram of 20-m hollow slab beam loading test

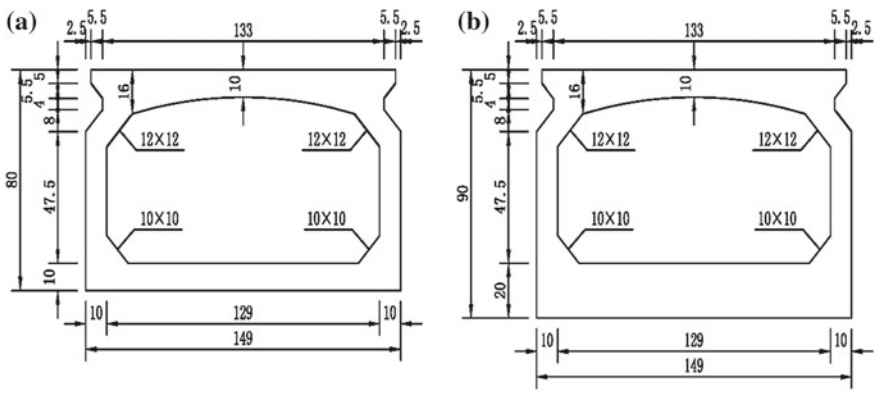


Fig. 2.4 Cross-section image of 20-m hollow slab beam. **a** Cross-section of midspan of mid hollow slab. **b** Cross-section of branch point on mid hollow span

Table 2.1 Measurement results of crack breadth

Bridge span No.	Crack position	Crack breadth (mm)			Changes in crack	
		Before loading	After loading	After unloading	After loading/ before loading	After unloading/ before loading
Third span on the left	Bottom of Slab Beam No. 3	0.150	0.171	0.158	1.14	1.05
	Bottom of Slab Beam No. 5	0.160	0.179	0.16	1.12	1.00

Table 2.1 presents the crack breadth of Slab Beam No. 3 and No. 5 before and after loading and after unloading. The results show that the changes in the crack width before and after loading were 1.14 for Slab Beam No. 3 and 1.12 for Slab Beam No. 5. Changes in the crack width after unloading and before loading are 1.05 for No. 3 and 1.00 for No. 5. Slab Beam No. 5 is thicker and more rigid at the bottom compared with No. 3. Thus, its longitudinal crack recovers completely. By contrast, Slab Beam No. 3 is thinner and less rigid at the bottom compared with No. 5. Thus, its longitudinal crack does not recover completely, indicating that No. 3 already sustains structural damage.

During the loading process (Fig. 2.5), as the load increases, the rigidity decreases because of the growth of the crack. As loading continues to increase, the structure shifts from a state of elasticity to a state of elastoplasticity, which slightly slows the reduction of structural rigidity. At the late stages of loading, the rate of rigidity reduction decelerates gradually and exhibits an almost linear relationship with deformation before reaching the maximum load bearing capacity.

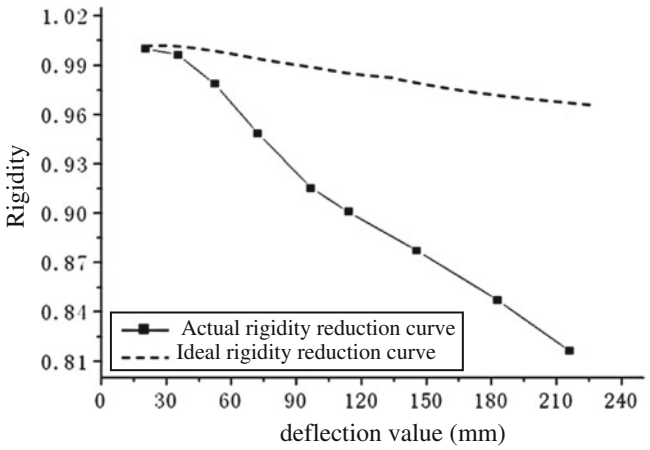


Fig. 2.5 Changes in rigidity in loading process

According to the failure test of width-optimized hollow slab beam structure, because the rigidity of the width-optimized hollow slab beam structure is small (primary factor), its fissure is prone to damage (secondary factor). This phenomenon is similar to the congenital immunodeficiency condition in humans, which renders them prone to acquired illnesses or complications induced from mild disease conditions. In particular, trunk highway bridges often sustain heavy load due to heavy traffic volume; moreover, when under overload, these structures shift from a state of elasticity to a state of elastoplasticity, which easily results in damage accumulation. Similarly, frequency used in telecommunication corresponds to a certain level of power. To achieve resonance point, frequency must be identical and power must be large enough. If frequency is identical but power is insufficient, then point of resonance cannot be achieved.

In summary, bridges with mid-to-small spans, small rigidity, and local deficiency are prone to accumulated damage, which causes unfavorable force and energy to be transferred to or concentrated on weak elastoplastic parts of the bridge. Regarding damage accumulation in structures, although the deformation and load bearing of structures in practice do not cause structural mutation, the effects of accumulated damage under repeated load expose trunk highway bridges to mutation when under load or deformation because of heavy traffic load and overload. Load-bearing or deforming structures gradually transition to a state of metastable equilibrium which is a precursor of a state of unstable equilibrium. Ultimately, structure failure occurs. Thus, prevention of structure failure should be strengthened. This is particularly crucial for structures with poor material property and those that experience large traffic flow, partial overload, and nonuniform distribution of load, which are conditions that exacerbate accumulated damage on these structures.

Example 2.2.2 A bridge has its top structure made of 4 × 20 m prestressed reinforced concrete simple support hollow slab. The bridge has a continuous deck and its bottom structure is composed of cylindrical pier and pile foundation. The layout of the bridge is shown in Fig. 2.6 and the standard cross-section of the bridge

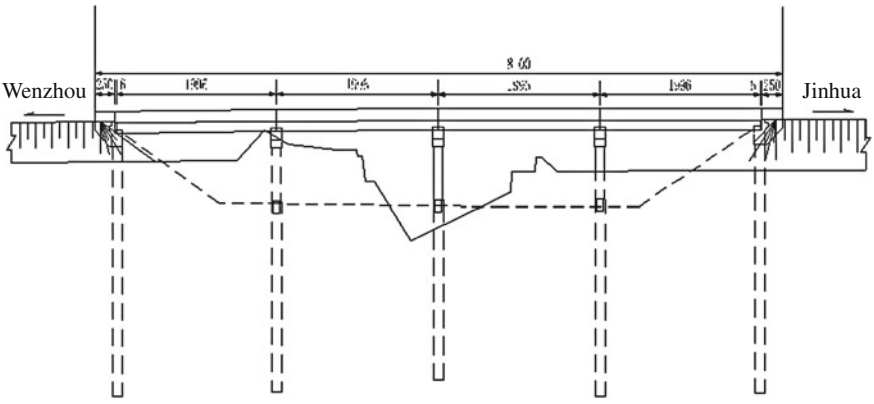


Fig. 2.6 Bridge layout

is illustrated in Fig. 2.7. A large transport truck has 30 axles, each weighing 20 t and placed 1.5 m apart from each other, yielding a total weight of 600 t.

Specific reinforcement measures are as follows:

(1) Beam slabs that do not meet stress requirements during transportation process are modified by pouring 5 cm-thick MPC (magnesium phosphate cement) composite material into the bottom of the beam (Fig. 2.8).
(2) Deck pavement is removed and reconstructed. After beam slab fissures are cleaned, high-strength grouting material is poured into the fissures and implantation bars are used for reinforcement (Fig. 2.8).

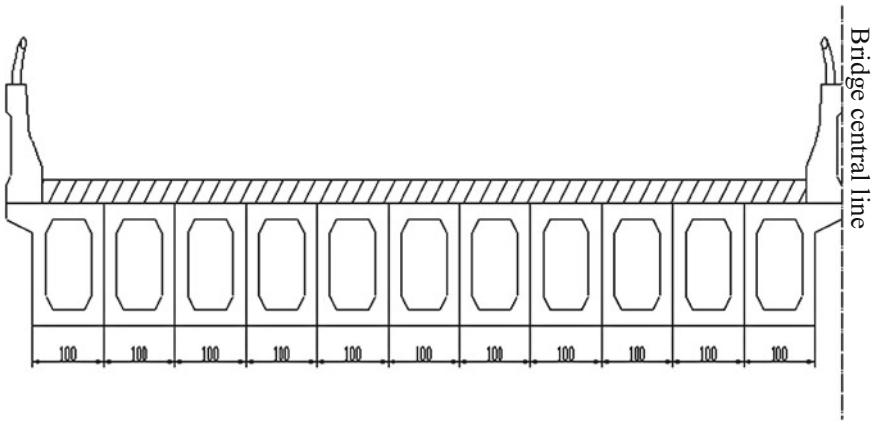


Fig. 2.7 Standard bridge cross-section

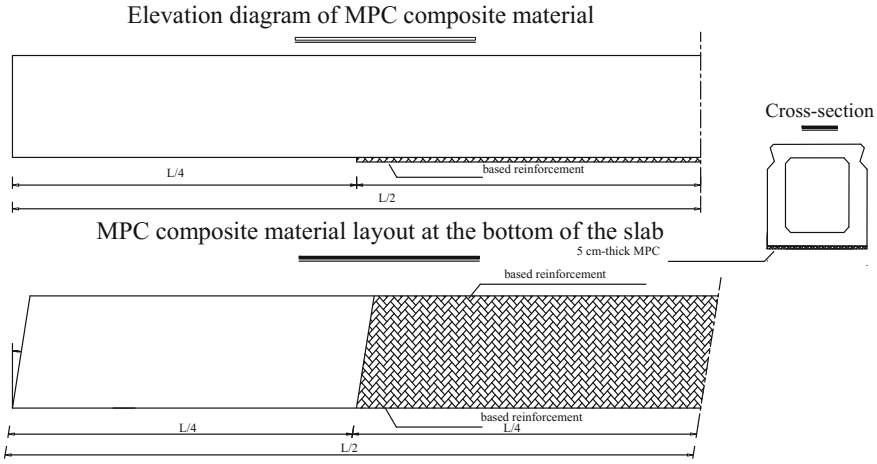


Fig. 2.8 Structural diagram illustrating the reinforcement of a bridge

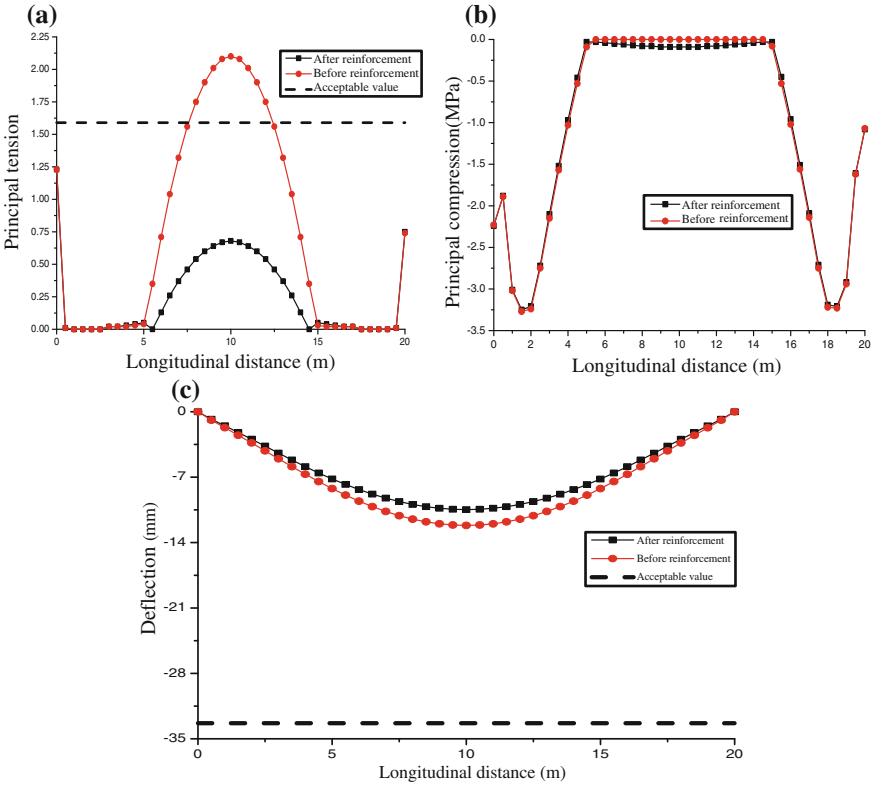


Fig. 2.9 Comparison of stress and deflection at the bottom of the beam before and after reinforcement. **a** Comparison of principal tension before and after reinforcement. **b** Comparison of principal compression before and after reinforcement. **c** Comparison of deflection before and after reinforcement

Figure 2.9 illustrates the calculation results of tensile stress, compressive stress, and deflection of the central line of the beam bottom slab before and after reinforcement. Positive and negative stress values represent tension and compression, respectively. Negative deflection value represents force in vertically downward direction.

Translation: After reinforcement; before reinforcement; acceptable value

Under special types of load, the bottom midspan of a beam slab structure before reinforcement exceeded the tension limit (as indicated by the central baseline in Fig. 2.9a) whereas it satisfied the requirement for vertical deflection. Under special types of load, the bottom of the reinforced mid beam slab exerted a principal tension that is smaller than that before reinforcement. Furthermore, the tension was smaller than was the regulated value.

Thus, bridge components should be comprehensively examined before subjecting them to special types of loads. Top parts of bridge structures should also be modified and reinforced according to designs to ensure vehicle safety and safe driving.

In summary, accumulated damage testing was conducted on a 20-m simple support hollow slab beam structure and heavy-duty transport theory analysis and testing of 20-m simple support hollow slab bridge reinforced with MPC composite material were performed. The results revealed that the 20-m hollow slab beam structure demonstrated small vertical rigidity, making it suitable for only vehicles that are within the standard general traffic load for ordinary highways. Such structure is not suitable for trunk highway bridges where heavy loads and overloads are common because of heavy traffic volume. This phenomenon is consistent with the scenario in which 20-m simple support hollow slab bridges on trunk highways, under heavy traffic loads and overloads, are prone to damage or failure, which influences operation safety.

2.2.2 Accumulated Damage Test on Bowstring Arch Bridge Structures

(1) **Scan test on boom steel wires for bowstring arch bridge**

A part of the deck of a half-through reinforced concrete ribbed arch bridge is a floating system. Presently, trunk highway bridges often sustain heavy traffic load and overload. In particular, some arch bridges collapse primarily because of boom failure. Because the deck system of bridge beams is a floating system that is supported by a single boom, short boom bears not only tension (included in calculation) but also bending shear force (excluded in calculation). Long–short booms deform structures to varying degrees, which causes nonuniform load bearing. Consequently, the strain energy generated from function conversion cannot be effectively dissipated, damaging the bridge structure. In addition, boom anchor areas of a deck system are severely corroded, which prevents force and energy from transferring to or concentrating on weak elastoplastic parts of these areas, thereby ultimately influencing the lifespan of the structure. The diagrams below illustrate a scan image of cable wires from a boom, which was removed from a bridge for replacement purpose. Figure 2.10a provides a section image of the undamaged part, and Fig. 2.10b is a section image of the damaged part. Comparing these two images reveals several damages in the reinforcement bar.

(2) **Static load and fatigue testing on bowstring arch bridge boom wires**

Table 2.2 presents the static load and fatigue test conducted on five bowstring arch bridge boom wires. The results are described as follows: (1) Because the corrosion on the wires has not reached an extent that weakens the strength on the cross-section of the wire, all old wires exhibit favorable static load bearing capacity. This indicates that static load on bowstring arch bridge boom wires is not the

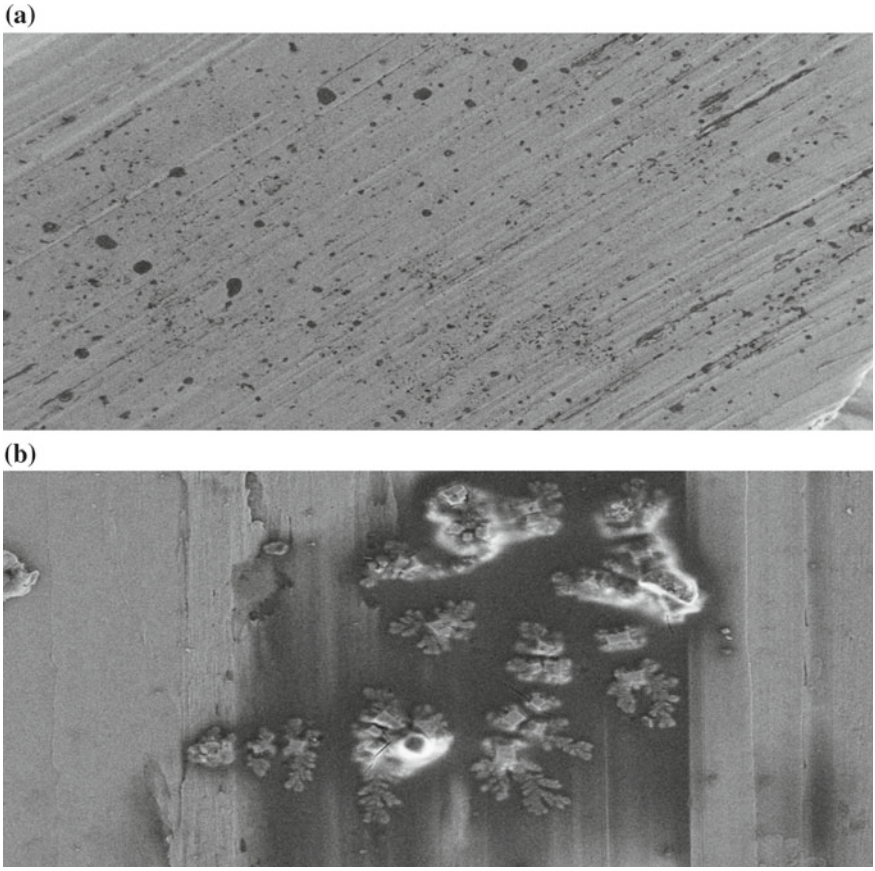


Fig. 2.10 Images of section scans. **a** Undamaged part. **b** Damaged part

primary factor controlling bridge designs. (2) Wires of Bridge No. 3 (bowstring arch bridge) on the national highway have the shortest fatigue lifespan, following by those of Bridge No. 2 (floating arch bridge) located on urban trunk roads. By comparison, wires of Bridges No. 4 and No. 5 have longer lifespan. Integrating the basic conditions and wire conditions of the five examined bridges shows that the bowstring arch bridges located on the national highway had the poorest fatigue performance. These highway bridges are often traveled by large cargo trucks. The floating arch bridges exhibited the second poorest fatigue performance because these bridges are frequently traveled by large coach and buses. This result indicates that the degree of fatigue on steel wires is strongly related to the traffic conditions on a bridge structure and the structural system of the bridge itself; and that the degree of change in axial stress is probably the predominant factor influencing the fatigue life of a boom. The wires of Bridges No. 4 and No. 5 that have not yet corroded performed well in resisting fatigue, whereas Bridges No. 2 and No. 3 that have corroded exhibited poorer performance in resisting fatigue. Therefore,

Table 2.2 Comparison of test results of five bowstring arch bridge boom

Bridge No.	1	2	3	4	5
Traffic condition	City, fewer heavy-duty vehicles	City, mainly buses	National Highway 104, more heavy-duty vehicles	Connecting line between Hangzhou-Ningbo Expressway and Yuyao, fewer heavy-duty vehicles	Provincial Highway 224, fewer heavy-duty vehicles
Boom safety coefficient	5.54	2.59	2.49	3.35	3.3
Boom corrosion	<1.0%	0.47%	0.49%	<1%	<1%
Boom static load test	All old wires exhibited favorable static load bearing capacity because the extent of corrosion in the wires is not sufficient to weaken the wire cross-sections				
Boom fatigue test	–	66.70%	41.70%	100%	100%

corrosion in wires might also influence the fatigue life of booms. This result indicates that fatigue in boom wires of bowstring arch bridge is likely the principal factor controlling design and that it is closely related to heavy load traffic and the structural system of the bridge. Furthermore, this fatigue problem is relevant to the suitability of bridge structure types and heavy load traffic on trunk highways.

The results shown in Fig. 2.10a, b and listed in Table 2.2 indicate that numerous operating bowstring arch bridges, specifically floating arch bridges, tend to exhibit fatigue damage and therefore break at the boom wire area because the overall rigidity values of those bridges are low. Subsequently, bridge safety is compromised. Therefore, this type of bridge is suitable for only vehicles that are within the standard general traffic load for ordinary highways. Such structure is not suitable for trunk highway bridges where heavy loads and overloads are common due to heavy traffic volume. This phenomenon is consistent with the scenario in which 20-m simple support hollow slab beams on trunk highways, under heavy traffic loads and overloads, are prone to damage or failure, which influences operation safety.

A large volume of test results regarding 20-m simple support hollow slab bridges and bowstring arch bridges, particularly floating arch bridges, revealed the following: Generally, a 20-m simple support hollow slab bridge is characterized by low rigidity; therefore, given that trunk highways are often subjected to heavy traffic loads and even occasional overloading, this type of bridge often demonstrates deformation incompatibility, which causes bridge damage to accumulate and concentrate on weak parts of the bridge structures. For example, the fissures of a 20-m simple support hollow slab bridge and the bottom parts of the short booms of a floating bowstring arch bridge aggravate

the damage accumulated on the weak parts of those bridge structures. Subsequently, the damage accumulates until it cracks the bridge and causes bridge failure, which alters the path of force transmission and state of load-induced deformation in the bridge structural system. Such changes result in discrepancies in the actual load-induced deformation and design load-induced deformation of the bridge structures. Given that trunk highways have no limits to loading and the bridges on these highways are not reinforced, trunk highway bridges are often subjected to heavy traffic loading and even occasional overloading, which ultimately can cause bridge reinforcement failure and bridge collapse as well as safety incidents.

2.2.3 Deformation Compatibility Control Problems in Bridge Expansion Device and Deck Paving

Example 2.2.3 DCC problems in bridge expansion device: The main bridge of a large bridge is a two-span suspension bridge with steel box girder. The bridge deck is a floating system. The bridge is located in a coastal area where typhoons frequently hit. Under wind and vehicle loads, bridge beams undergo horizontal and vertical angular deformation and torque-based displacement. The modular bridge expansion joints of the bridge do not satisfy beam deformation requirement. Under fan-shaped displacement and compression, the mid-beam steel undergoes irrecoverable plastic deformation. The bottom load-bearing support is damaged and will eventually cause subsidence or fracture in the mid-beam steel, which severely impacts traffic safety, as shown in Fig. 2.11. This type of damage has also been observed in the modular bridge expansion joint used in similar bridges in China. Because adverse conditions induce main beam displacement or large deformations, expansion joints either undergo constrained deformations or additional deformations. Thus deformation incompatibility in the main beam and expansion joint or inside the expansion joint may generate greater constrained or additional forces, which accumulates stress-induced damage on expansion joint materials. Subsequently, the lifespan of the expansion joint is shortened, leading to risks of accidental safety-related incidents. Therefore, transfer or concentration of adverse forces and energy toward weak elastoplastic areas of bridge structures must be avoided.

Modular bridge expansion joint restrictor can control the maximum expansion value at an expansion joint. A bridge expansion joint (Fig. 2.12) has six restrictor devices installed on two ends (one device each at the two ends and the center) to effectively control the maximum expansion value of a bridge expansion joint. Thus, the volume of expansion can be uniformly distributed, thereby mitigating the damage on bridge expansion joints (Fig. 2.12).

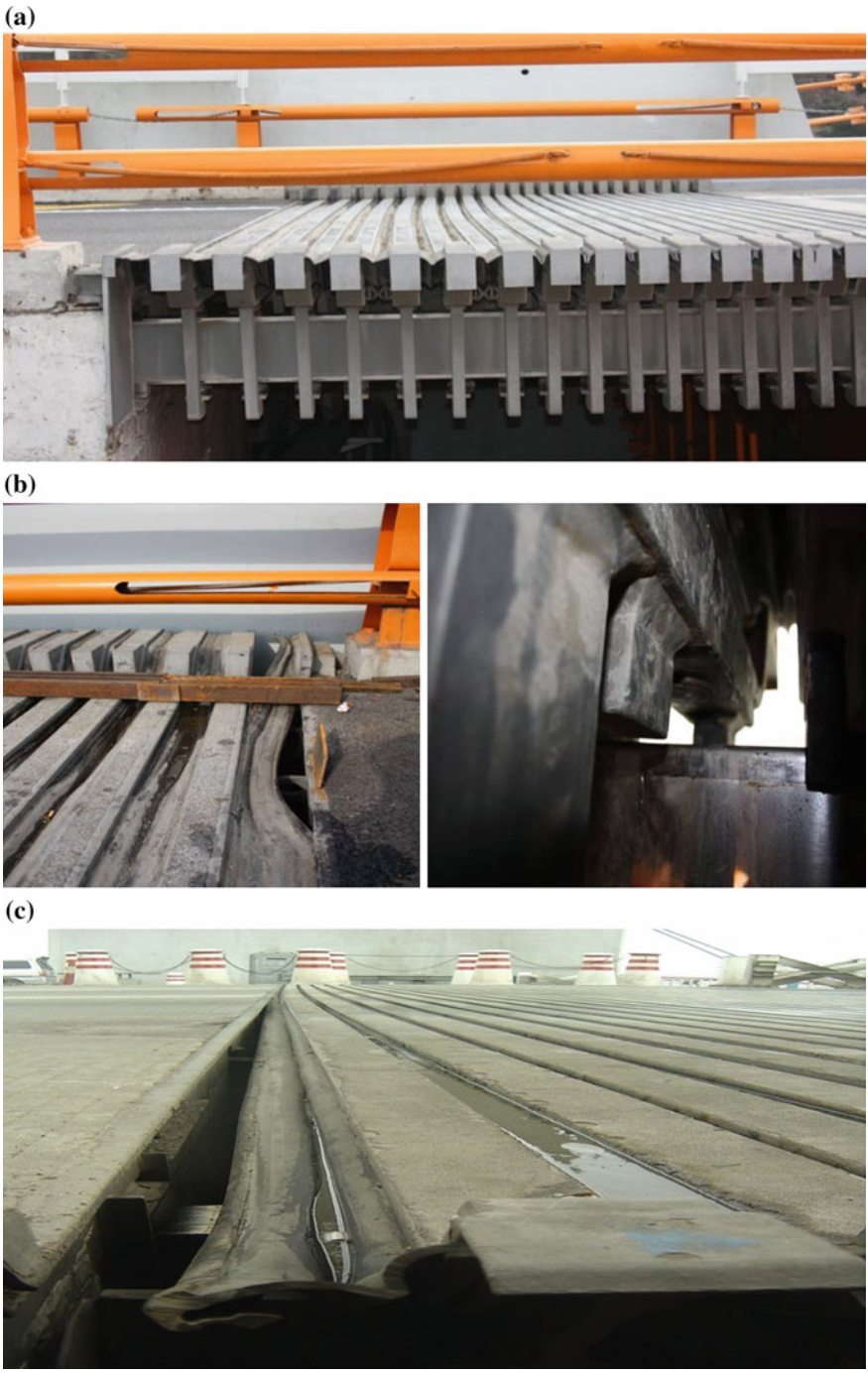


Fig. 2.11 Photographs showing the damage on bridge expansion joint

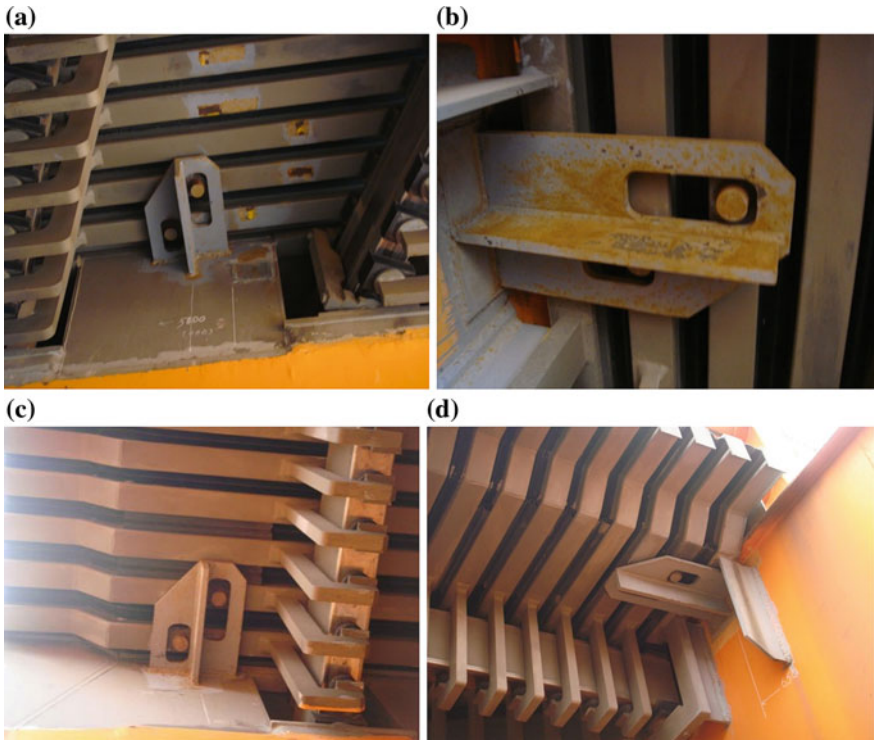


Fig. 2.12 Restrictor improvement measures implemented on a bridge expansion joint

Example 2.2.4 DCC problem in deck paving: Bridges built in the early 90s are characterized by decks that are made of asphalt concrete, which suffer damage easily (Fig. 2.13). Management units must conduct deck maintenance at least twice a year, which consumes considerable resources. Analyzing the root cause of damage to deck asphalt concrete reveals that the design of previous bridges focused excessively on lightweight characteristics. Such optimized lightweight bridges exhibited inadequate rigidity and excessive vertical deformation, thereby causing deck failure. Based on these inadequacies, a solution to constantly breaking decks that require constant repair is to increase the vertical rigidity of the bridge and mitigate vertical deformation.

To solve the aforementioned problem from an alternative perspective, focus can be placed on increasing bridge vertical rigidity, rather than on only deck repair and maintenance, to solve the fundamental problems regarding deck maintenance. Numerous methods can be employed to mitigate bridge vertical deformation such as changing structural systems or increasing horizontal contact and vertical bending rigidity.

Compared with concrete decks, steel bridge decks are easily damaged primarily because of the localized inadequate rigidity of the steel deck plate. Deformation in



Fig. 2.13 Road failure test involving inadequate vertical rigidity

the layer containing asphalt concrete pavement and deformation in the steel deck plate are incompatible.

As mentioned previously, asphalt concrete pavement of steel bridge decks is prone to damage. To solve this problem, a novel composite deck made of orthotropic steel place and ultrathin, ultrahigh performance reinforced concrete can be used to strengthen bridge decks, thereby preventing steel deck pavement from damage and protecting steel structures from fatigue and cracks, as shown in Fig. 2.14. Furthermore, the key to this prevention approach is to raise steel bridge deck rigidity, reduce deck deformation, and keep the maximum level of deck deformation below the maximum level of deformation in asphalt concrete pavement layers or ensure that the maximum level of deck deformation and maximum level of deformation in asphalt concrete pavement layers are compatible.

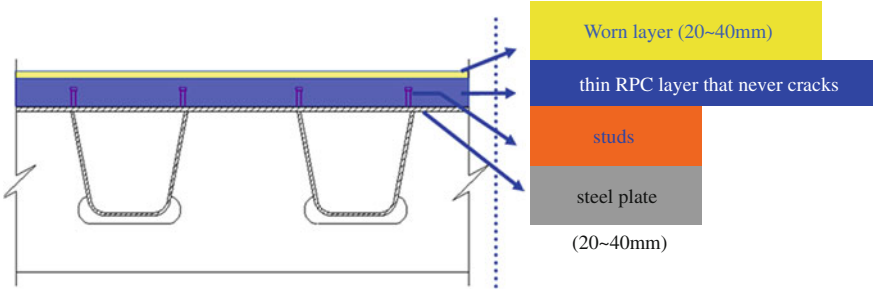


Fig. 2.14 Composite deck made of orthotropic steel plate and ultrathin and ultrahigh performance reinforced concrete

Compared with general steel decks, the new composite deck incorporates a thin layer of reactive powder concrete (RPC). RPC is a type of cement-based composite material that features ultrahigh strength, ultrahigh toughness, and high durability. RPC is a type of high performance reinforced concrete that can be attached to steel deck plate by using welding and studs. The Humen Pearl River Bridge is made of this novel composite deck. Through finite element calculation and full-scale model testing, the composite deck demonstrates deck plate rigidity 40 times greater than that of a general deck. In addition, the horizontal tension on the steel plate is reduced by 78% and the tension on the deck plate and weld in the longitudinal rib are reduced by 68%. The results indicate an effective solution to the problem that deck pavements are prone to damage and steel structures are prone to fatigue and fracture. These observations also suggest that composite decks made of orthotropic steel plate and ultrathin and ultrahigh performance reinforced concrete demonstrate extremely high application value in steel bridge designs.

2.2.4 Deformation Compatibility Control Problem Associated with Bridge Safety in Mountain Areas

Mountain areas largely comprise meandering rivers and unfavorable hydrogeological conditions. Mountain highway bridges are exposed to risks of external load as well as risks of water-related problems. To solve these two problems, not only is systematic thinking required but the link between events and objects must also be established to ascertain the coupling and mutual effects between the two problems. Concerning water-related problems in highway bridges, a number of considerations must be taken into account, including sudden water flow impact, uncertainty in position and depth of erosion, and the coupling and mutual effects between water-related risk and stress-related safety. Therefore, to ensure the safety of bridges in mountain areas, stress-related safety and water-related risks of bridge structures must be considered in designing of bridges. The physical analysis of a bridge design must be conceptually correct and the quantitative analysis must be mathematically correct. To ensure the quality of the design, relevant engineering calculations and quantitative analyses should be approximately accurate within acceptable ranges of approximation. Furthermore, effective skills and management procedures should be adopted to ensure construction quality. These approaches facilitate solving major problems at the design and construction stages. Just like people resolve their health concerns by checkups, nutrition and medication, bridge structures with minor problems can be improved through maintenance and management, whereas major problems or compatibility problems are resolved only through reinforcement or modification. People manage their health by maintaining good bodily health and developing healthy lifestyles. They adjust their health regimens when they develop mild illnesses, and for major illnesses, they undergo treatments or surgeries.

Therefore, the design, construction, maintenance, and management of bridge structures in mountain areas should be based on the stability of equilibrium state of bridge structural systems, and adopt equilibrium, stable equilibrium, and stable equilibrium and DCC theories to analyze and determine the safety of the bridge structure. For general circumstances, theoretical calculation and analysis are required. By comparison, analysis of special circumstances requires not only theoretical calculations but also integrate methods involving effective structural systems, construction methods, suitable support and protection, as well as process control. Consequently, stable equilibrium and DCC in the entire engineering works of bridge structures can be achieved.

Based on the aforementioned discussion, the following recommendations are proposed for improving problems associated with bridge safety in mountain areas: (1) The scientific nature of bridge engineering should be elucidated from structural engineering perspective and factors that influence bridge safety, including natural disasters, overload, state of bridge structures, and effective protection measures should be comprehensively investigated. (2) Minor potential problems in bridge structures (e.g., Bridges No. 1, 2, and 3 as listed in Table 2.2) should be prevented by strengthening repair, maintenance, and management and by eliminating bridge-related risks. (3) Major potential problems in bridge structures (e.g., Bridges No. 4 and No. 5) should be addressed by adopting corresponding measures of driving restrictions, comprehensively analyzing the cause of bridge risks, employing effective reinforcement or modification plans, and strengthening reinforcement or modification of at-risk bridges to prevent safety-related incidents.

Example 2.2.5 Recommendation for Reconstruction of Bridges on Meandering Rivers in Mountain Areas

Meandering rivers in mountain areas are characterized by sudden water flow impact and uncertain erosion position and depth. Investigation of an arch bridge on meandering river in a mountain area and bridge compatibility problem (Fig. 2.15) revealed the following findings: arch bridges have lower compatibility compared with beam bridges; expansion foundations have lower compatibility compared with pile foundations; and effective abutment and coast protection must be developed.

According to the fact that engineering structures must simultaneously satisfy stable equilibrium and DCC requirements and according to an investigation of an arch bridge on meandering river in a mountain area and bridge compatibility problems, bridge reconstructions must consider the following factors: (1) Beam bridge is the recommended option. (2) Pile foundation is the recommended option. (3) Revetment of a certain length must be built on the two sides of an abutment. In other words, engineering structures must simultaneously meet stable equilibrium and DCC requirements and avoid considering only stable equilibrium requirements and neglecting DCC requirements.

Example 2.2.6 Recommendation for Restoration of Special Large Bridges in Mountain Areas

A bridge (Fig. 2.16) was constructed to serve as a temporary bridge for ensuring smooth traffic flow. The bridge is a two-tower two-span suspension bridge with 210



Fig. 2.15 Investigation of an arch bridge on meandering river in a mountain area and bridge compatibility problems

m-long main span and bridge load of 20 t. According to Fig. 2.16, the main beam is connected only to a Bailey steel beam support at the bottom, which yields not only insufficient vertical rigidity but also inadequate horizontal rigidity and torque-based rigidity. The original design probably focused mainly on the effect of vertical load, neglecting the effect of inadequate rigidity, which leads to increased secondary stress on the main beam, increased stress on bridge boom and main beam connection joint, as well as accumulated damage on bridge components such as the main beam and boom (these types of failure are frequent in highway bowstring arch bridges). Suggestions for bridge restorations are proposed as follows: (1) Increasing the height of Bailey steel beam to raise the vertical rigidity of the main beam; (2) increasing the horizontal connection between the top and center parts of the Bailey steel beam to form a space frame and increase the horizontal rigidity and torque rigidity of the main beam; (3) changing the fixed joint at the connection between the boom and main beam to a hinge joint to overcome the problem regarding increased secondary stress on the connection joint; and (4) adding safety protection device on top of the main beam. Main beam designs must consider not only vertical load problems but also the secondary stress and damage accumulation caused by structure deformation incompatibility. In other words, engineering structures must simultaneously meet stable equilibrium and DCC requirements while preventing the situation that considers only stable equilibrium requirements and neglects DCC requirements (Fig. 2.18). Comparison of the load–deformation



Fig. 2.16 Before and after bridge damage



Fig. 2.17 Load–deformation state of the Jingshajiang suspension bridge (completely different to the bridge shown in Fig. 2.16)

models of the Jingshajiang (Fig. 2.17) suspension bridge and the current bridge shows considerable difference, and this difference must be addressed in bridge designs.

According to the book, Jianzhu Jiegou de Oumi: Li de chuandi yu xingshi (the Mystery of Architectural Structures: Transmission and Forms of Forces; Kawaguchi et al., translated by Xiaodun Wang) as shown in Fig. 2.19, to prevent deformation generated by uneven loading and wind-induced vibration, a reinforced



Fig. 2.18 Horizontal restrictive rope-based suspension bridge in Switzerland and Taiwan

beam with improved rigidity must be included in large-span suspension bridge designs. Uneven lateral deformation involves a complex mechanism (which is consistent with the normal load–deformation state of the horizontal restrictive rope-based suspension bridge in Switzerland and Taiwan shown in Fig. 2.18 and with the states of damaged and undamaged bridge as shown in Fig. 2.16).

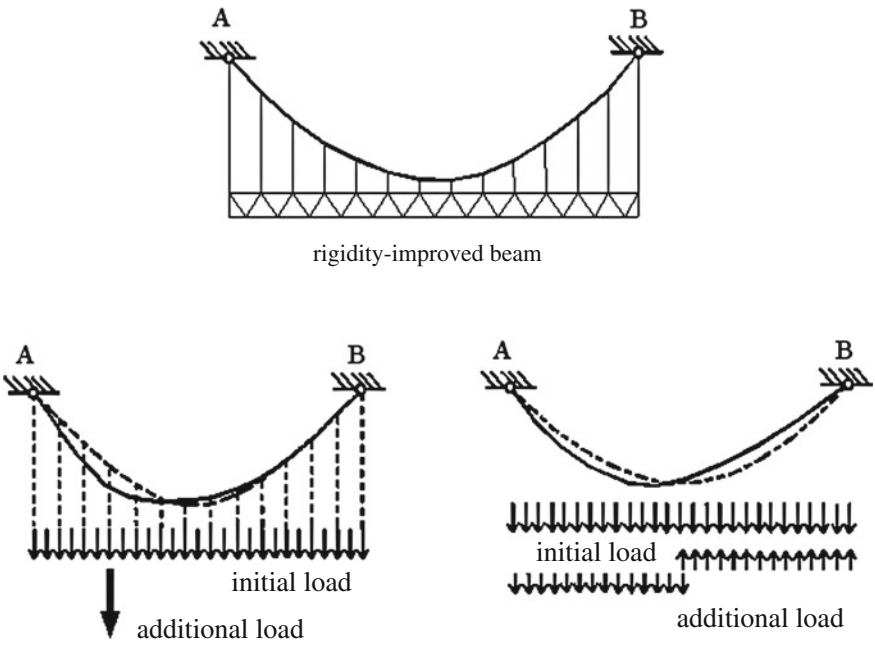


Fig. 2.19 Schematic diagram illustrating the direct influence of different suspension bridge reinforced beam rigidity on the load-bearing capacity and deformation of the main rope

2.3 Application Effectiveness of Deformation Compatibility Control Method in Tunnel Structure

Previous underground construction works often neglect "temporal and spatial effects," that is, the validity of load-bearing structure layers, the timeliness of load-bearing structure layer formation, and spatial stability. In particular, spatial stability and DCC during construction process **cannot be used to control force transmission, and such inadequacy may negatively affect force transfer, leading to collapse-related incidents**.

The key to using DCC method is to ensure that force is transmitted via the **designed path** in tunnel structures to control force transmission and prevent unfavorable force transfer. **Improving designs and construction according to structure DCC methods** and emphasizing the effective tunnel excavation and protection are conducive to controlling the plastic deformation or loose deformation of surrounding rocks to minimize collapse arch and maximize load-bearing arch. Thus, **ensuring that force is transmitted via the designed path and controlling effective force transfer can prevent surrounding rock mutation and collapse**.

In simple favorable geological environments, stable equilibrium in underground engineering can be achieved easily. As long as correct concept of physics is understood, whatever theory or construction method selected does not matter. For underground constructions in adverse geological conditions and complicated engineering environment, insightful ideas and correct engineering protective measures are needed to explain related laws and clarify uncertainties. Otherwise, it can influence the path of force transmission or transfer in a structural system, thereby changing the stable equilibrium state of the structure and even creating new unfavorable equilibrium state.

When surrounding rock stability is low (approximately **10–20%** consists of soil or fragments, and blasting is not required), excavation should proceed in conjunction with construction of supporting and protecting structures, and the excavation length for supporting measures must be controlled within 1–2 m to prevent the deformation and collapse of the surrounding rock. The key to this process is the effectiveness of load-bearing structure layer, particularly spatial stability during construction (analysis of the mechanics and DCC must be done to control plastic deformation or loosening in surrounding rock, and the reduction of self-bearing capacity).

When surrounding rocks are stable and rock bodies are rigid (**approximately 70–80%** and smooth blasting is critical), the construction process typically involves excavating the tunnel cross section and then constructing supporting measures. Furthermore, when conditions allow, the whole excavation can be completed before the supporting measures.

2.3.1 Deformation Compatibility Control Measures for Mountain Tunnel

The design and construction of mountain tunnels generally focus on the smooth blasting, shotcrete-bolt support, and monitoring and measurement problems associated with the New Austrian Tunneling method (NATM). However, in far too many cases, numerous other factors are not seriously considered, including the effectiveness of load-bearing structure layers and the timeliness and spatial stability (in particular, the spatial stability during construction) of load-bearing structure layer formation (i.e., spatiotemporal effect). Irrespective of the design calculation method used, construction methods and process control measures should be based on the stratum structure method (corresponding to the "rock supporting theory") to generate the collective effects of stratum and supporting structures and achieve stable equilibrium and DCC. Subsequently, related risks can be eliminated to ensure the safety of load-bearing process during construction works (Figs. 2.20 and 2.21).

A collapse in a mountain tunnel forms a large hollow space. Mountain tunnels have lower ground deformation requirements than other structures. Therefore, pipe roof supports and inserted plates can be used to form scaffolding support. When reinforcing a mountain tunnel that has suffered a partial collapse, the hollow space caused by that collapse can filled with lightweight materials to control its expansion

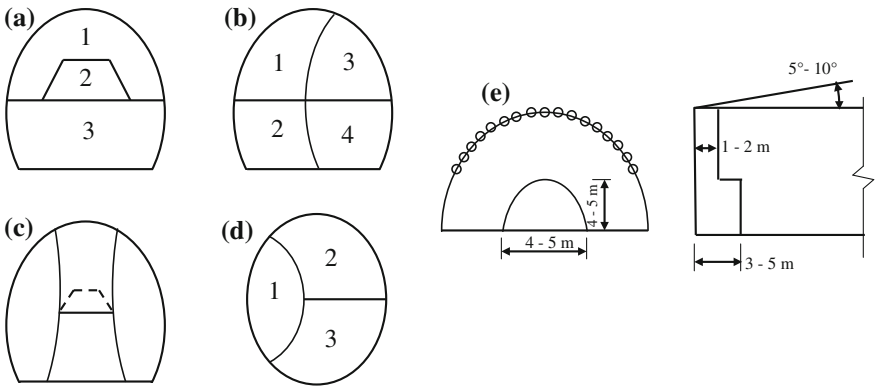


Fig. 2.20 Controlling of spatial stability of supporting structures for excavation of mountain tunnels in unfavorable geological conditions. *1* When surrounding rock stability is low (contains soil and fragments, and blasting not required), excavation is necessary in conjunction with erecting supporting structures, and the length of vertical excavation support structures must be controlled within 1–2 m to prevent surrounding rock deformation and collapse. Please see diagrams *b*, *c*, *d*, and *e*. The key to this process is the validity of load-bearing structure layer, particularly spatial stability during construction (mechanics and deformation control). *2* When surrounding rocks are stable and rock bodies are rigid (blasting is required), the construction process typically involves excavating tunnel cross-section and then building supporting structures. Furthermore, full face excavation can be completed when conditions allow

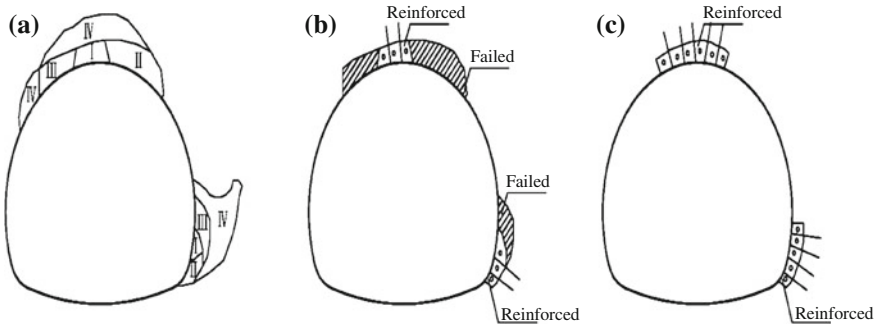


Fig. 2.21 Evolutionary process of controlling spatial stability of supporting structures for excavation of mountain tunnels in general geological condition. Schematic diagram illustrating the evolutionary process of load–deformation state and force transfer or transmission in supporting and load-bearing structures for tunneling construction

and prevent chipping while reducing support load in order to limit the adverse effects of the hollow space. The aforementioned measures accord, in nature, with the energy increment criterion in a stable system: $\Delta U > \Delta T$ (where ΔU denotes work done by system resistance against force and ΔT denotes work done by loading). The path of this relationship involves force passing through the pipe roof support and inserted plate scaffolding and acting as a protective force to increase ΔU, which then passes through the lightweight material to control expansion and prevent chipping of the hollow space, thereby mitigating support load and reducing the work done by load ΔT $(\Delta T = P\Delta S_1 + W\Delta S_2)$. Subsequently, unfavorable force and energy are prevented from transferring to or concentrating on weak parts of the structure.

Figure 2.22 shows the collapse of Yongjia Tunnel. When the tunnel had been excavated to a tunnel face at section K16+183, the ceiling of the tunnel collapsed. The length of the collapsed area measured approximately 11 m, the horizontal width was 10 m, and the height was 22 m, yielding an estimated volume of roughly 2420 m^3. A surface geological survey revealed a hidden fault near the tunnel face at section K16+183. The fault runs along the northeast direction and bends toward the northwest direction. A number of sandwiched layers containing fragmented rocks were observed. Some of these layers were particularly thick. The fragmented rock section exhibited low stability. The thickness of the remaining strata at the collapsed location was 4.0 m; the chamber formed by the collapse was 3.5 m high, with collapse debris accumulating at the bottom, exhibiting signs of continued fragmentation and collapse.

As a countermeasure, a pipe roof support was extended across the collapsed area and foam concrete was injected into the cavity above the pipe roof support. Subsequent operations were performed once 70% of the designed concrete strength was reached. The foam concrete prevented the continued collapse of fragmented rocks inside the chamber; it also alleviates the load on top of the pipe roof support, thereby ensuring the safety of the surrounding rocks and supporting structures.

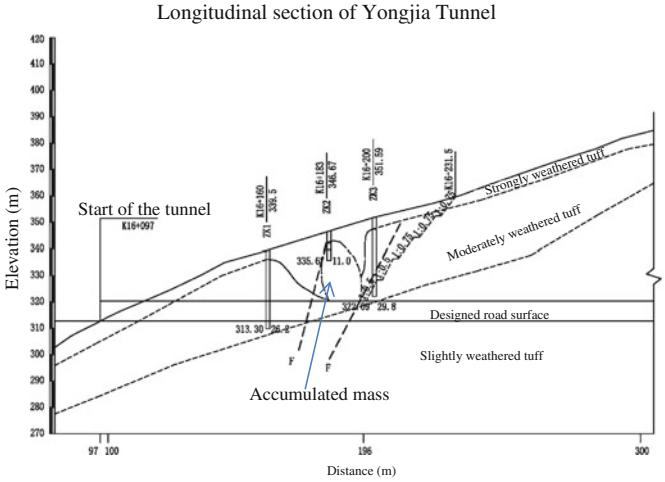


Fig. 2.22 Sudden collapse of roughly 2420 m^3 of the Yongjia Tunnel during excavation process

2.3.2 Deformation Compatibility Control Measures for Shield Tunneling

To date, most engineering designs and engineering consultations merely focus on the load applied after the completion of the entire structure. Structures are designed and feasibility verifications are performed according to regulations. Component designs are based on accepted canons of design. This type of design method is feasible when the form of structure and engineering environment are simple. However, when structural form and environment are complex and variable, the effects of load changes on structural stability cannot be accounted for. Shielding construction involves highly integrated technologies and complex construction skills. In addition, geological environments also involve complex variables. The design analysis of overall shield tunnel structure must be integrated with structural measures, design methods, and actual construction skill control in order to ensure the stable equilibrium and DCC of shield tunnels, thereby achieving design and construction goals. The mechanical properties of tunneling are significantly affected by the construction process. The essence of tunnel design and construction is to ensure the timeliness and effectiveness of stability control for soft surrounding rocks.

In shield tunneling, factors such as excessive excavation, shield shell thickness, and shield tail gap cause the formation of a stratum space that is larger than the outer space of the tunnel segment, which generates a gap between the tunnel segment and the stratum layer. Such a gap must be grouted in order to control the stratum deformation and the position of the tunnel segment. The grout can be classified as hard grout and inert grout according to whether the grout is mixed with

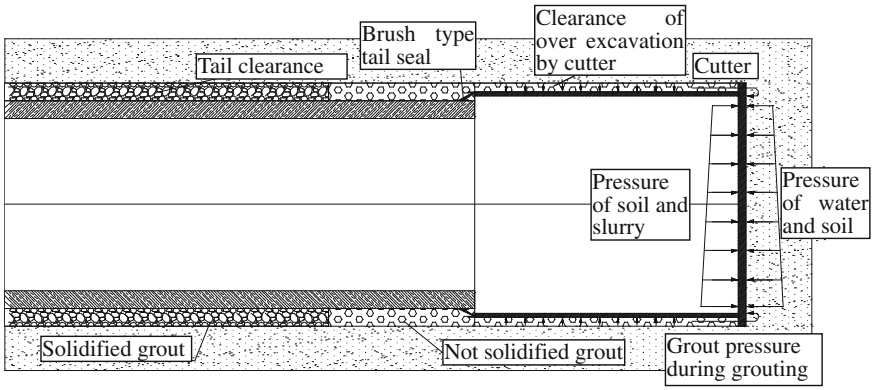


Fig. 2.23 Schematic diagram of shield tail gap and grouting

cement or other forms of gelatin. The initial strength and final strength of hard grout are all higher than those of inert grout. However, the grouting pumps and grouting pipelines used for hard grout must satisfy stricter requirements than those used for inert grout do. In China, to save on grouting equipment and grout cost, grouting is usually performed with inert grout that has low initial strength and final strength. As shown in Fig. 2.23, if grout cannot solidify immediately during synchronous grouting, the grout flows into the soil chamber of the shield machine through the gap between the shield shell and surrounding rocks. Fluid grout with strong fluidity causes large pressure variations inside the soil chamber due to the weak pressure-maintaining ability of the screw excavation approach for an earth pressure balance shield (EPBS). Large pressure variations substantially influence the stable control of the excavation surface.

Therefore, synchronous grouting should adopt hard grouts that solidify quickly and have higher initial strength. This way, the solidifying grout can fixate the tunnel segment within a short time so that the tunnel segment can transfer the applied load to the stratum under the effect of shield thrust, thereby restricting cyclic deformation in the tunnel segment (ellipsoidal deformation easily subjects circular tunnel segments to adverse stress conditions and concurrently causes ground deformation). Subsequently, the tunnel formed meets the designed linear requirements and a protective layer is formed outside the tunnel segment. Meanwhile, gaps are filled to eliminate the aforementioned factors that disturb the equilibrium state, facilitate the achievement of stable equilibrium and DCC in the stratum and tunnel segment, and ensure the safety and quality of shield tunneling.

According to DCC as shown in Figs. 2.24 and 2.25, tunnel segments are made of rigid materials and soil bodies are semiflexible. The initial strength of inert grout is associated with flexible materials; thus, rigidity incompatibility easily destabilizes shield tunnel segment or renders soil deformation incompatible. Hard grout has higher initial strength, making it equivalent to a semirigid and semiflexible material; it helps an interacting shield–stratum system achieve stable equilibrium and DCC.

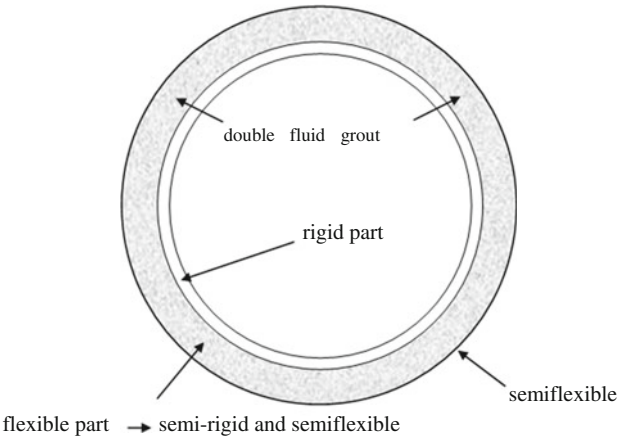


Fig. 2.24 Schematic diagram of injection of hard grout at the cross section of the shield



Fig. 2.25 Homogenous elastic compartmented tires have better control than do rubber pneumatic tires over DCC and uniform load-bearing capacity of tire inner ring

Alternatively, a construction method in which double fluid grout is poured after synchronous injection of inert grout can be employed; the principle behind this approach is similar to the pouring of hard grout.

Excavating soft strata layer yields a collapsing space, altering the initial state of stability and load-bearing conditions of the strata. To maintain the initial load-bearing and deformation states of the strata, support must be provided in advance or the strata should be filled with materials that are stronger and more rigid than are undisturbed soil. This way, complete filling and solidification requirements can be fulfilled to effectively control stratum deformation. For relatively stable strata in a nonload-bearing water environment, concrete pump can be employed to transport, in a synchronous manner, fine sand mixtures that are similar to mortar, are just as heavy as undisturbed soil, and exhibit favorable pumpability, to fill shield shell and shield tail gaps.

Soil consolidation of strata containing muddy soil or viscous soil with low penetration coefficient easily occurs when the shield reaches a certain distance. At this point, the tunnel segment should be supplemented with group to eliminate the

effect of strata consolidation. This way, stable equilibrium between the structure and soil body can be maintained to satisfy the stable equilibrium and DCC requirements for engineering structures.

Example 2.3.1 Second injection of double fluid grout: Grout can be classified into two types according to its plastic state retention time: grout that can maintain in plastic state for 5–30 min is referred to as special plastic grout; and solidification grout can be further classified into slow solidification grout, which has extremely low initial strength and requires more than 30 s to solidify, and instant grout, which has high initial strength and takes less than 20 s to solidify.

Plastic grout can be used in grouting of tunnel segments. As the area of injection increases, the grout is injected sequentially. Despite low injection pressure, the grout can still fill a large area because the grout is a plastic consolidated grout that gradually moves forward as the injection proceeds until the shield tail gap is completely filled. Because the grout is highly viscous, it does not easily mix with the surrounding soil. This type of grout can effectively fill up to the maximum level. During shield construction, synchronous grouting generally adopts single-fluid grout. In underground environment where water is abundant, this type of grout cannot achieve favorable filling performance; it cannot be restricted to a certain area and demonstrates low consolidation strength. Therefore, single-fluid grout is not ideal for strata filling.

Second injection of double fluid grout is advantageous in that fluidity is retained during the process and injection is performed only in the specified area. In other words, double fluid grout contains instant consolidated, plastic grout that facilitates achieving region-specific injection. When grout is used to fill the shield tail gap, it is hoped that the grout can solidify as quickly as possible and that the grout can be just as strong as the soil bodies in the surrounding rocks. Therefore, the initial strength of double fluid grout is mandated to achieve target compression strength of 0.1 MPa after one hour. If the solidification time of slow solidification grout is too short, the grout will lose its fluidity before the injection is completed, thereby causing unfavorable filling effects.

According to DCC as shown in Fig. 2.24, tunnel segments are made of rigid materials and soil bodies are semiflexible. The initial strength of inert grout is associated with flexible material; thus, rigidity incompatibility easily destabilizes shield tunnel segment or renders soil deformation incompatible. Double fluid grout has greater initial strength, making it equivalent to a semirigid and semiflexible material; it helps a system achieve stable equilibrium and DCC.

After synchronous grouting of shield is performed, additional double fluid grout is injected at regular interval to form a grout fracture framework that resembles the hoops of a wooden barrel. This framework is beneficial for balancing the load exerted on hinge-connected tunnel segment and increasing the load-bearing stability of hinge-connected tunnel segment. In addition, prestressing can be applied to increase stability even though theoretical analysis that does not consider DCC cannot solve the stability problem. The balanced and unbalanced load of molded shield tunneling and whether the tunnel is consistently constrained by radial water and soil

pressure are similar to the principle of load-bearing mechanism of empty hooped and nonhooped barrel. When empty hooped and nonhooped wooden barrels are placed with their axes parallel to the ground and vertical downward force is applied, the load-bearing capacities of these wooden barrels may differ distinctly. This model can be used to simulate the exposure of tunnel surroundings to unbalanced load. Barrel hoops exert a radial constraint on the barrel itself; such force is equivalent to the homogenous water and soil pressure applied to the tunnel in the stratum. Barrels without hoops can be compared to tunnels without homogenous constraint in the areas surrounding the tunnels; its stress-induced deformation is incompatible, and it seems to bear load in localized areas. Adjusting the tightness of the barrel hoop serves to adjust the magnitude of the constraint exerted on the entire barrel. The constraint of the outer hoop around the barrel limits the deformation of the barrel body. Each wooden plate makes up the entire barrel. A barrel has a large outer volume and a smaller internal volume. Each plate touches each other on the side and is connected to each other to collectively provide counter force. Thus, the barrel remains stable under load and exhibits DCC; in addition, it is capable of withstanding high pressure. Conversely, each piece of wooden stave of a wooden barrel without hoops does not experience the constraint of hoops and therefore does not generate prestress force. In addition, deformation of each wooden plate cannot exert constraining effect; thus, once a single piece of plate experiences a load and generates incompatible deformation, it detaches from the entire structure, which disrupts the entire equilibrium system of the barrel under load. For example, a vertically assembled circular tunnel segment (Fig. 2.26) has an inner diameter of Φ5.5 m, outer diameter of Φ6.2 m, length of 1.2 m, and thickness of 0.35 m. Single circular tunnel segment weighs 19.3 t, indicating that its upper half portion weighs 9.65 t. Thus, if the bottom half of the tunnel segment has no effective ground radial supporting force to constrain the overall deformation of the tunnel segment, even if the entire tunnel segment is affected by only the upper half of the segment, such influence may impede the vertical circular formation of the tunnel segment.

When the shield passes through key pipelines and buildings, a second injection of Grout B is performed on the tunnel segment. By adjusting the solidification time of the grout, the shield tail gap can be effectively filled and the ground surface deformation can be controlled. Figure 2.27 illustrates a comparison of filling single-fluid and double fluid grouts to control ground surface deformation.

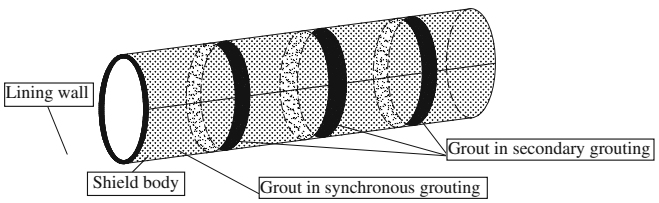


Fig. 2.26 Analytical diagram depicting the stability of the hinge-connected tunnel segment in soft stratum

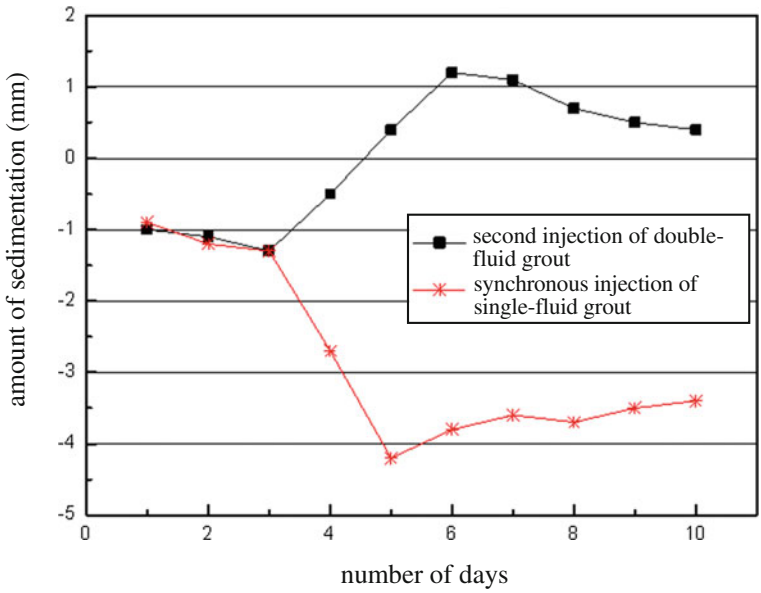


Fig. 2.27 Comparison of filling single-fluid and double fluid grouts to control ground surface deformation

2.3.3 Application Effectiveness of Deformation Compatibility Control Method in Metastable Tunnel Construction

1. **Entrance of Tunnel Collapse Process**
   The original design of a tunnel involves a 390 m-long left tunnel, which has a two-lane road, and a 362 m-long right tunnel, which has a three-lane road, as shown in Fig. 2.28. Affected by the mountain fracture zone, mining goaf,

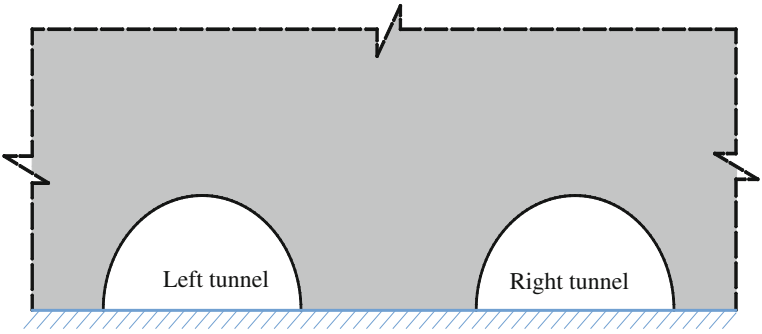


Fig. 2.28 Layout cross section of a tunnel

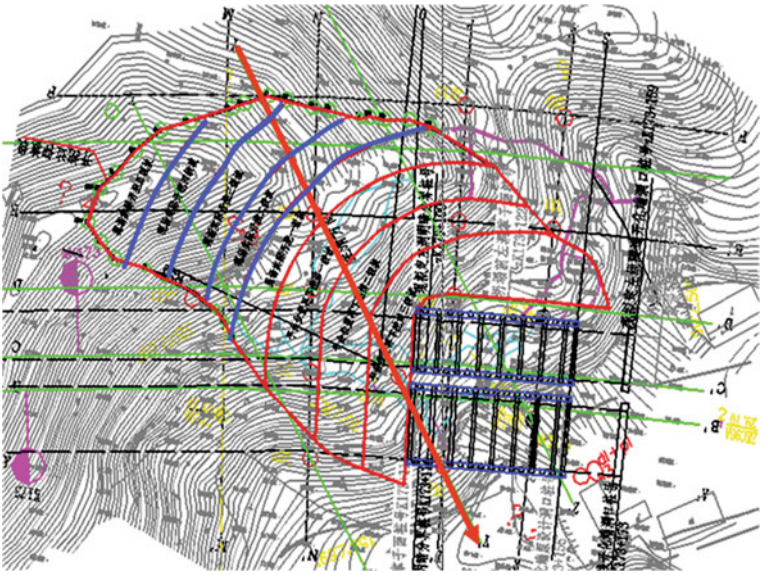


Fig. 2.29 Plane configuration of a tunnel opening and indications of slump

asymmetric rock pressure, short distance, and torrential rain due to typhoon, the mountain and left tunnel collapsed on August 22, 2013 at 20:35, and the right tunnel collapsed at 23:10. The mountain slid downward by approximately 15 m. The sequence of the collapse is depicted in Figs. 2.29 and 2.30: Left tunnel collapsed → Mountain lost its stability and slumped → Right tunnel collapsed → Mountain continued to slide until it reached stability. According to analyses of collapse processes and factors such as differences in the current topology and original topology and surface cracks, the collapse was of moderate size.

2. **Slump Process Analysis**

   (1) When the excavation length was 9 m (ZK173+151) at the upper bench of the left tunnel, excavation began at the middle bench. At this time, cracks appeared on the heading slope of the left tunnel entrance, indicating weak support in the early period and no instant ring formation. Therefore, there was a lack of support to resist against the pressure from the slope of the tunnel entrance.

   (2) Subsequently, the left tunnel was excavated to section ZK173+140.5. The empty hole at the supporting arch foot was filled; a steel support was established inside the hole; cracks were observed at the umbrella arch and initial support in the tunnel. Observation results indicated that, the original support inside the left tunnel was weak; an overbreak had possibly occurred; rings did not form instantly; the support was not able to resist the pressure and thrust from the slope at the tunnel entrance.



Fig. 2.30 Process of slump at a tunnel entrance

(3) The right tunnel was excavated to sections YK173+146-YK173+137 and initial support was built. However, excavation of the right tunnel was to be avoided when the left tunnel was not completely stable because both tunnels exerted adverse effects on each other.
(4) Continual excavation of the right tunnel and building supporting structures accelerated unfavorable deformation to its maximum limit. Care should be taken with regard to this aspect in the future.

(5) Typhoon-induced torrential rain aggravated the pressure and thrust from the slope at the tunnel entrance, causing the collapses of the left and right tunnels one after another.

3. **Recommendations on Supplementary Measures for Design and Construction**

The following measures could be supplemented to the original design and construction measures to facilitate the stable equilibrium and DCC analyses of excavation and support constructions during the excavations of the tunnel entrances and the tunnels.

(1) The loose mountain slope at the opening of the tunnel may have reached its maximum equilibrium state. Thus, when an empty hole is discovered, back filling of grout and addition of anchor frames at the slope should be performed to control the pressure and thrust exerted by the slope, thereby increasing the stability of the slope at the tunnel entrance.
(2) At the initial stage of construction, double layer supporting structure, small depth excavation, immediate closing off of inverted arch should be adopted. Thus, the supporting structure can bear most of the pressure and localized thrust exerted by the slope.

4. **Countermeasures after the collapse**

Based on the analysis of the process of tunnel slump, countermeasures (Fig. 2.31) are proposed as follows:

(1) Repair the heading slope and the slope near the entrance and build protective supports from the crown to the toe; up to the height of the slope base, subsequent excavation methods can be used, accompanied with a crown



Fig. 2.31 The reinforcement and tunnel excavation and establishment of supporting structures on the slope near the opening of a tunnel

beam top on a supporting pile or a backfilled top protruding from an open tunnel. Excavate the slope and simultaneously erect supporting structures; control the increment of height to equal the required height for constructing a row of anchor bolts (anchor ropes); and closely monitor the geological conditions of the exposed surface during excavation and, where necessary, install small pipes for grouting.

(2) Dig a 39 m deep excavation method-based open tunnel and a 38 m deep large excavation-based open tunnel in the left and right tunnels, respectively, erect 60 protective piles, with lengths of 22.8 or 25 m, around the foundation pit, and adopt impact drilling method to drill holes.

(3) After the construction of protective piles is completed around the foundation pit, commence the pouring of top crossbeam, crown, and brace. First excavate the earth stone area at the foundation pit of the right tunnel and establish four rows of supporting structure around the foundation pit: two rows of reinforced concrete supporting beam above the pit and two rows of temporary steel pipe support below the pit. Subsequently, excavate and erect supports level by level (i.e., build support on one level immediately after the excavation at that level).

(4) After the construction of the excavation method-based open tunnel is completed in the right tunnel, immediately backfill the open tunnel in the right tunnel. Thereafter, immediately commence the construction of the open tunnel at the foundation pit of the left tunnel while commencing the construction of hidden tunnel in the right tunnel. When the secondary pouring of the hidden tunnels in the right tunnel reaches a distance of 50 m, commence the excavation of hidden tunnels in the left tunnel until both left and right tunnels are completed.

2.3.4 Application Effectiveness of Deformation Compatibility Control Method in the Construction of Soft Plastic-Flow Soil Tunnel

1. **Basic Conditions**

A large portion of a tunnel is a mountain tunnel with 300 m of its length located along a riverside. Shallow underground excavation is required to cross the soft plastic-flow soil stratum. However, using shield construction is uneconomical. How should the tunnel be designed and constructed to ensure construction safety and the safety of surrounding architectures? Figures 2.32, 2.33 and 2.34 depict the plane layout of the tunnel crossing area, cross section of the geological profile, and samples of muddy, powder clay samples. Figure 2.35

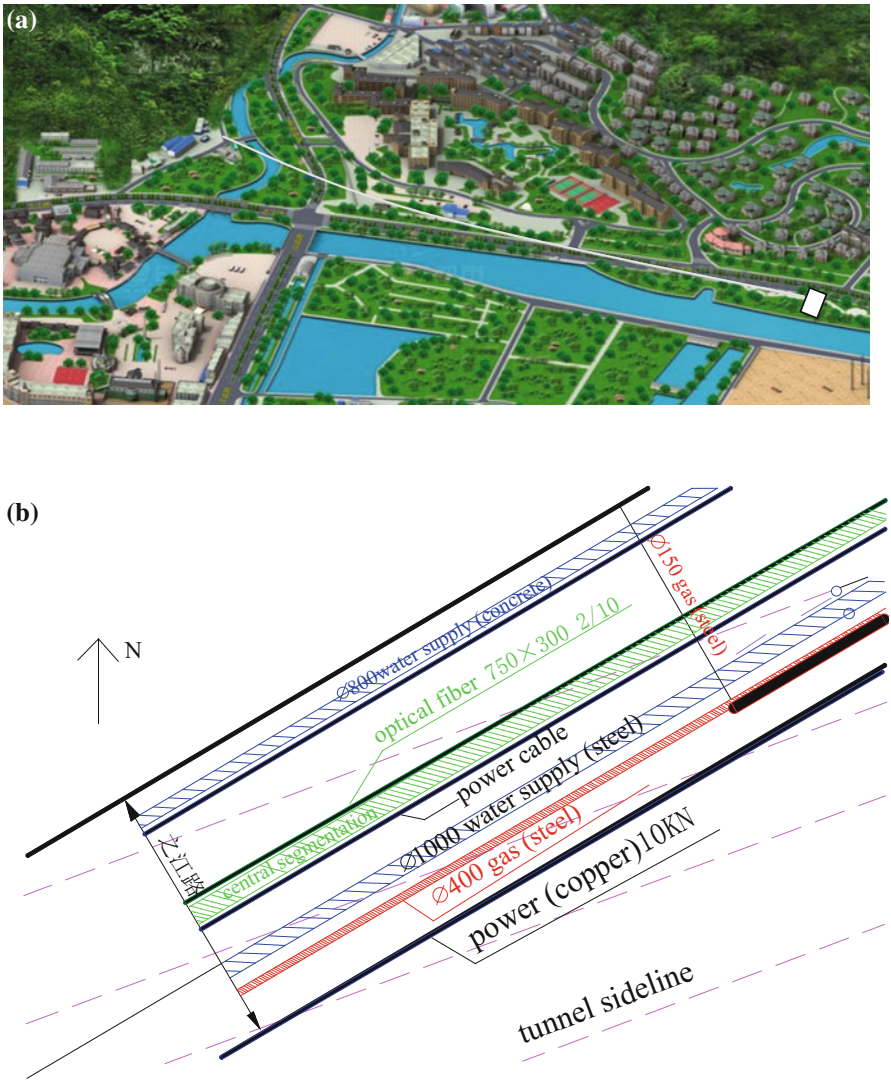


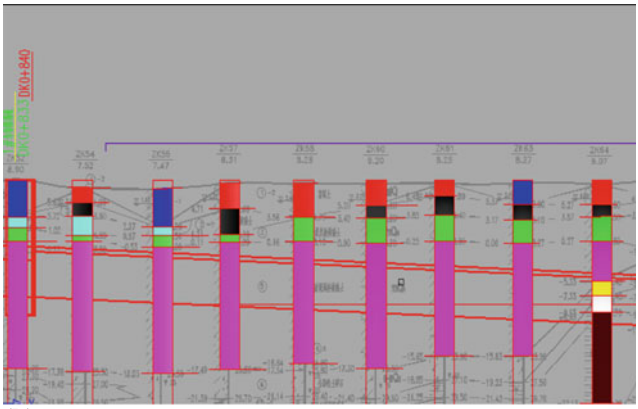
Fig. 2.32 Floor plan of a segment of pipeline distribution and overall crossing zone of a tunnel

presents the procedure of excavation and supports of Grades IV and V surrounding rocks of the tunnel.

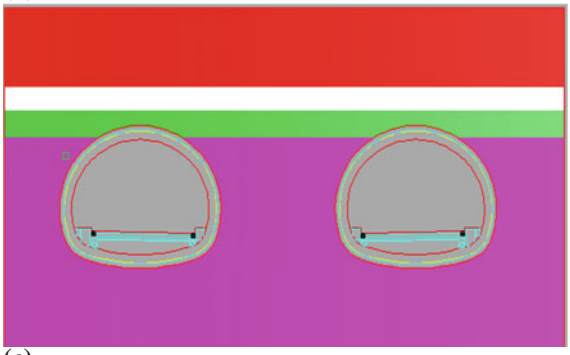
2. **Engineering Difficulties**

(1) The underground water level in the tunnel is high. The standard underground water level is 4.4–5.2 m. Loss of underground water occurs during tunnel excavation, which lowers the stability of the rock body, thereby causing ground subsidence. Underground water prompts the soil to undergo secondary stress redistribution after the initial support is established; such

(a)



(b)



(c)

Layer No.	①—1	①—2	①—3	②—1	②—2	③	⑤	⑥
Name	Mixed fill	Plain fill	Pond mud	Powder clay	Powder clay	Muddy powder clay	Muddy powder clay	Viscous soil and fragmented stones
Color fill								
Layer No.	⑫—1	⑫—2	⑫—3	⑭—2	⑭—3	⑮—1	⑮—2	⑮—3
Name	Viscous soil and fragmented stones	Strong weathered argillaceous siltstone	Moderately weathered argillaceous siltstone	Viscous soil and fragmented stones	Strong weathered fine siltstone	Full weathered fine siltstone	Strong weathered tertiary basalt	Moderately weathered tertiary basalt
Color fill								

Fig. 2.33 Cross-section diagram of a segment of geological environment in the crossing zone of a tunnel



Fig. 2.34 Muddy, powder clay samples obtained from a working well

redistribution leads to deformation in the arch frame and increases the requirements for tunnel water prevention and water discharge.

(2) Protecting underground pipelines and temporary constructions is challenging. Tunnel crosses under a section of road, which comprises ductile iron water supply pipe with a diameter of 1000 mm, reinforced concrete water supply pipe with a diameter of 800 mm, and gas pipeline of 400 mm in diameter. These pipes pose extremely high requirements for the control of ground subsidence. In addition, whether tunnel subsidence can satisfy the subsidence requirements of ground pressure pipelines is a major challenge in tunnel construction. The tunnel crosses under water diverging culvert below Qiantang River, intersecting with the culvert. The ceiling of the tunnel is 6.92 m apart from the culvert. Tunnel excavation may induce excessive deformation in the culvert, causing culvert leakage and flooding in the tunnel.

(3) Tunnel crosses under urban roads where a cover layer is thin and soil quality is low. The tunnel crosses a section of the road that is composed of Grade VI surrounding rocks. The primary strata under which tunnels cross are composed of thick layers of plastic-flow, saturated muddy and powder clay, mixed with few thin layers of silt. The strata are classified as soft soil with similar soil properties. These types of strata are low in strength, highly thixotropic, and highly compressive. Excavation of such soil easily induces creep and a large amount of deformation; it has no self-supporting stability after excavation.

Therefore, the initial design and construction plan or improvement plans for such tunnel cannot meet the conditions surrounding the tunnel excavation line and even ensure the stability of tunnel face during the

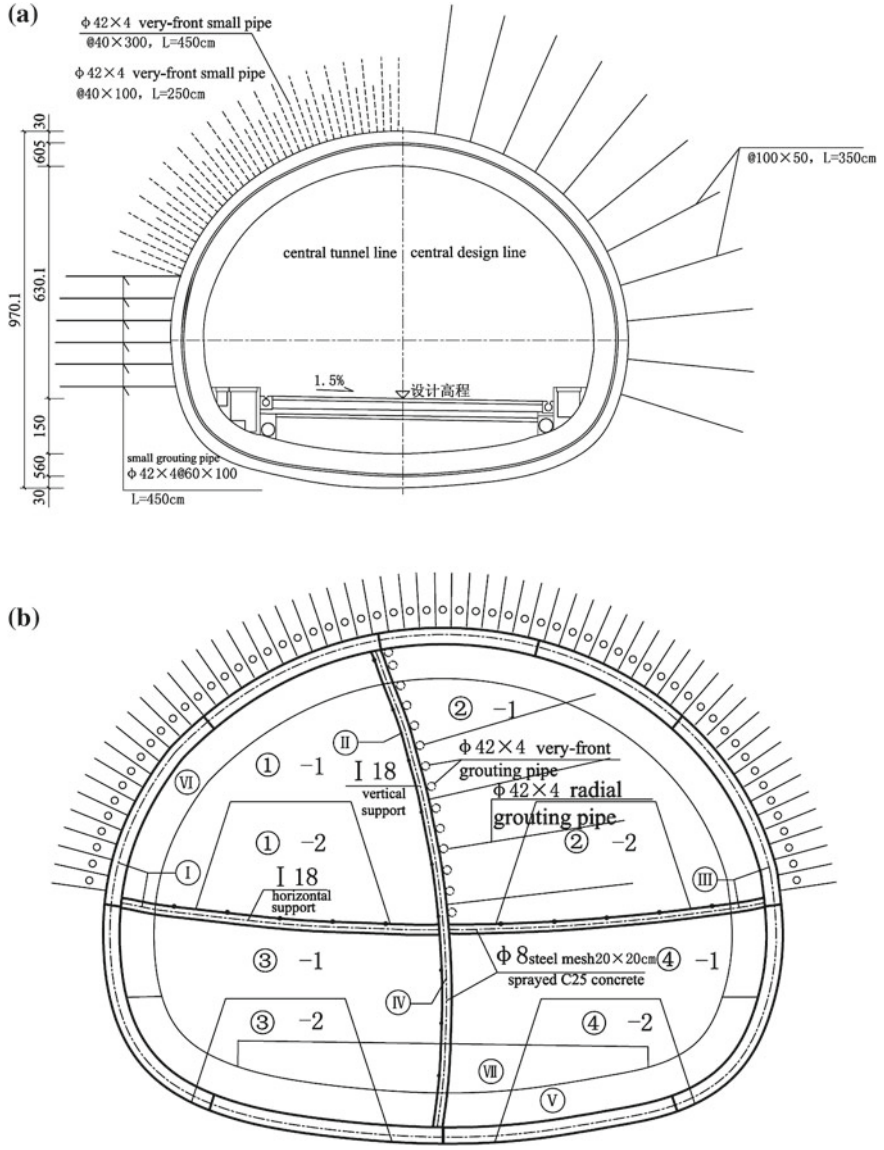


Fig. 2.35 Procedure of Levels IV and V excavation and support erection on the surrounding rocks of a tunnel

construction process. This process might pose construction risks, which negatively affect the protection of underground pipelines and temporary constructions on a segment of the crossing zone of the tunnel. Caution should be taken with regards to these risks. Please refer to Fig. 2.35 **for details**.

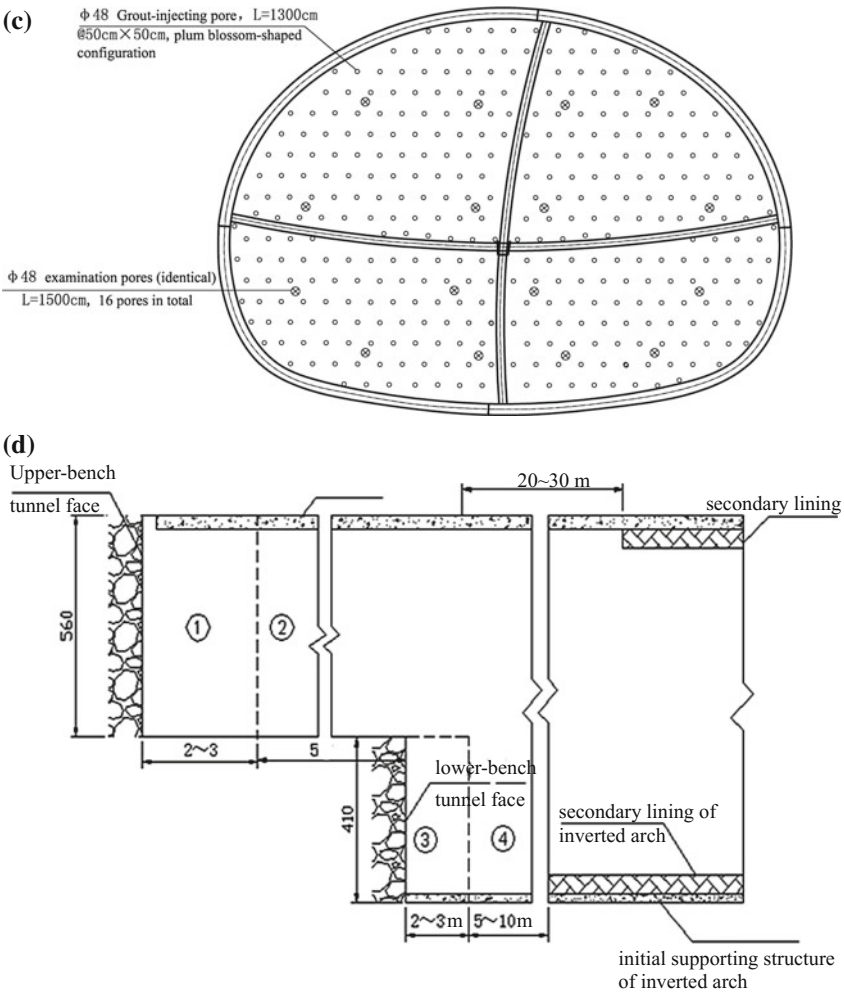


Fig. 2.35 (continued)

3. **Exploring Initial Tunnel Design and Construction Plan or Improvement Plans**

(1) Phase 1: Cracks observed on the intermediate wall

Excavation began at Mark-I west line by using the CRD method. Underground excavation began at K0+792.6 m, with excavation of No. 1 pilot tunnel already reaching K0+804 m, for an accumulated excavation length of 12 m.

On April 30 at 18:00, tunnel face in section K0+804, a quarter of the area of the right pilot tunnel on Mark-I west line, collapsed. A quarter of the area of the left pilot tunnel is situated at section K0+802. At K0+801, two vertical



Fig. 2.36 Diagram illustrating vertical steel pipe support

cracks were observed on the intermediate wall in the tunnel, one of which extended to the base of the top pilot tunnel. Currently, construction work has been shut down, and concrete was sprayed onto the tunnel face to seal the cracks. Subsequently, steel pipe horizontal supports were set up by attaching the pipes at the "waist" area of the tunnel, as shown in Fig. 2.36.
The ground surface of the west-line tunnel registered an accumulated maximum subsidence of 141.95 mm. From 17:30 on April 30 to 6:30 on May 1, a new subsidence depth of 21.78 mm was recorded, subsiding at a rate of 1.68 mm/h on the central axial line in the tunnel. Between 6:30 to 13:00, the ground subsided further by 11.84 mm, at a rate of 0.91 mm/h, indicating a stable trend on overall.
The top of the arch of the west-line tunnel registered an accumulated maximum subsidence of 14.5 mm.

(2) Phase 2: Continual development of deformation
Following the previous deformation in Phase 1, ground deformation has been controlled and stabilized by reinforcing the tunnel face with grout, installing steel pipe supports, and systematically injecting grout through small pipes. The current deformation was induced by a subsequent excavation after the previous deformation was stabilized.
Regarding tunnel excavation improvement method, one part of the construction has been conducted according to a six-step excavation method, with one part being based on the original four-step excavation, raising it by 1.7 m, as shown in Fig. 2.37.
During excavation, a stepped center core method is used with the center core length being 0.5 m, advancing length of 0.5 m/day. The steel supports are connected by joints at the boundary of the excavation steps, as shown in Fig. 2.37.

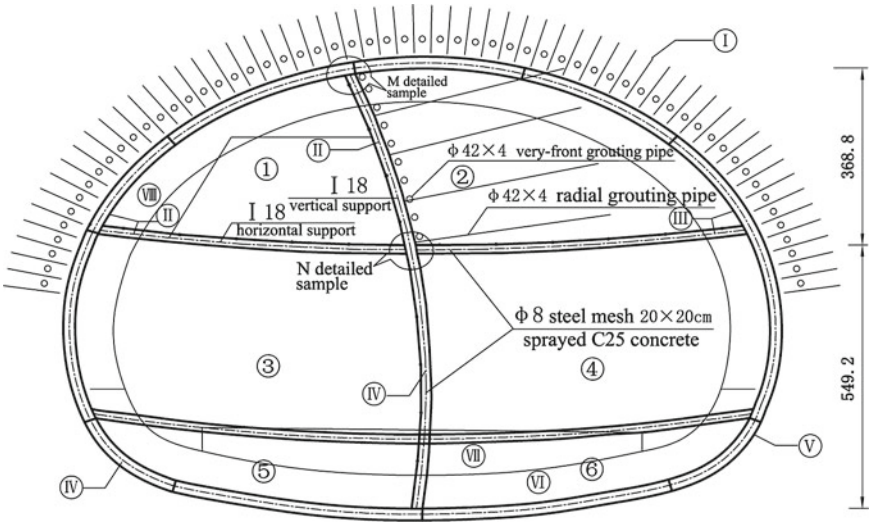


Fig. 2.37 Excavation method of a tunnel

(1) Construction of large-scale lead pipe roof, which has been completed during the construction of the tunnel entrance;
(2) Small lead pipes of 1.5 m long with intervals of 4.5 or 3 m, as shown in Fig. 2.38.
(3) Tunnel face reinforcement
Tunnel face was reinforced after the first large deformation by using small grouting pipes with a length of 9 m placed approximately 50 cm apart. The grouting method was whole pipe grouting.
(4) Execution of initial support and system support installment according to the original design plan
After the first deformation, the maximum ground subsidence was located about 2 m behind the tunnel face. The point of maximum



Fig. 2.38 Arrangement of very front small pipes

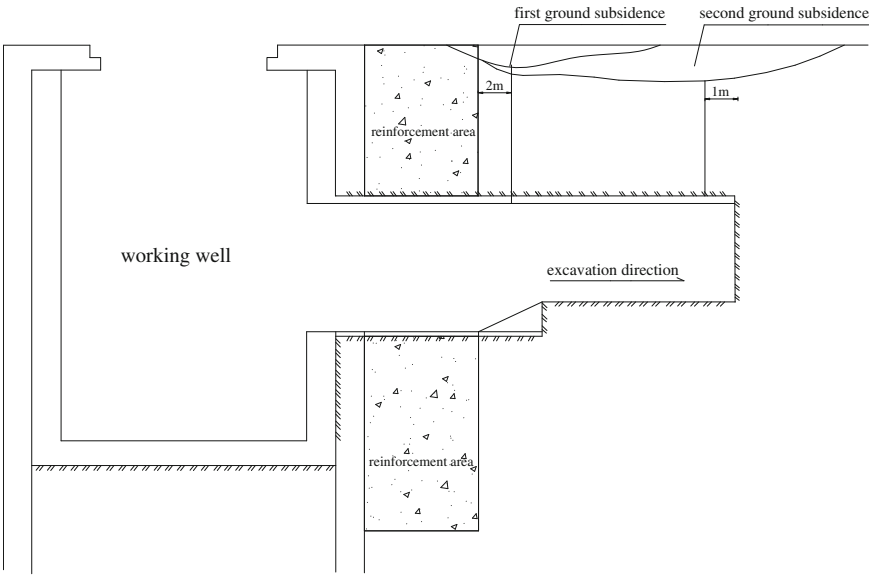


Fig. 2.39 Subsidence curve

subsidence moved toward the tunnel face to approximately 1 m behind the new tunnel face. Figure 2.39 illustrates the ground subsidence curve.

Cracks in the tunnel were primarily found at the connection joint of the steel arch frame located in the waist area of the tunnel chamber. This area had a large bending torque. Deformation in the connection joint was caused by tension on the inner side, causing the reinforced concrete to fracture.

(3) Grouting of soft plastic-flow soil tunnel could not guarantee the surrounding stability of the tunnel

Onsite core sample drilling at Pit No. 1 was completed, obtaining core samples from three holes. However, cores sample drilling of two holes had failed. The core sample from the other hole is shown in Fig. 2.40. The hole was located within 2.9 m of the tunnel face, and the sample indicated favorable grouting effect. At 7.9 m, the soil exhibited low strength and plasticity, indicating low self-stabilizing capability. Weak grouting effect was observed in the middle section, where soil exhibited soft plastic-flow state.

According to the core samples, grouting effect was improved after grouting method was improved; however, the grout exhibited poor homogeneity (core samples were obtained from three holes, and core samples were successfully obtained from only one hole). Favorable grouting effect was observed on the tunnel face, whereas the middle section exhibited poor grouting effect where the grout material was not clearly observed.

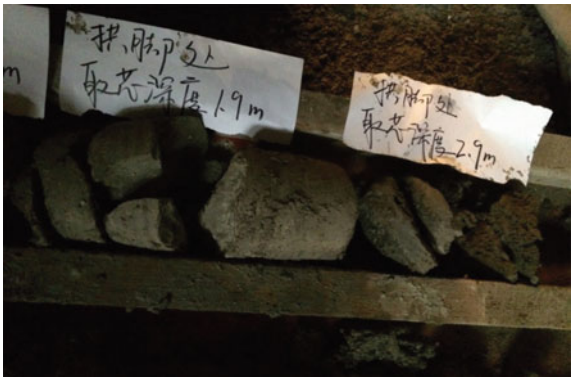


Fig. 2.40 Core sample within 2.9 m of the tunnel face

4. **Recommendations for Tunnel Design and Construction**
   The initial design and construction plan or improvement plans for such tunnel cannot meet the conditions surrounding the tunnel excavation line and even ensure the stability of tunnel face during the construction process. This process might pose construction risks, which negatively affect the protection of underground pipelines and temporary constructions on a segment of the crossing zone of the tunnel. Whether surrounding rocks satisfy constraints or whether the initial state of the surrounding rocks is effectively maintained can be considered to discern whether underground engineering structures meet DCC conditions. If DCC conditions are met, then the stress–deformation state of the structure in practice is consistent with that of the design structure. If DCC conditions are not met, then the stress–deformation state of the structure in practice differs from that of the design structure, which easily results in various types of problems, including unexpected problems or safety risks. Therefore, the mechanical principles underlying the stability of the surroundings of a tunnel and tunnel face during shield construction can be referred to ensure stable tunnel surroundings and tunnel face during excavation works. Moreover, various types of initial supports can be used to bear loads, such as using surrounding steel inserted plate supports specific to lead pipe roofs; injecting grouts to tunnel face; improving excavation and support construction methods; and employing steel arch frames and jet grouting. Alternatively, a lead support of a horizontal jet grounting pile can also be used to improve the surroundings of the tunnel and tunnel face stability. Please refer to Figs. 2.41, 2.42 and 2.43 for details.
5. **Implementation Plan: Ground Reinforcement by High-Pressure Jet Grouting Pile**

   (1) High-pressure jet grouting pile design parameters
   High-pressure jet groutind piles on the ground surface can be used to improve soil strength and increase soil mechanical performance. On the basis of previous improvement effects on soil in similar strata, the soil in a

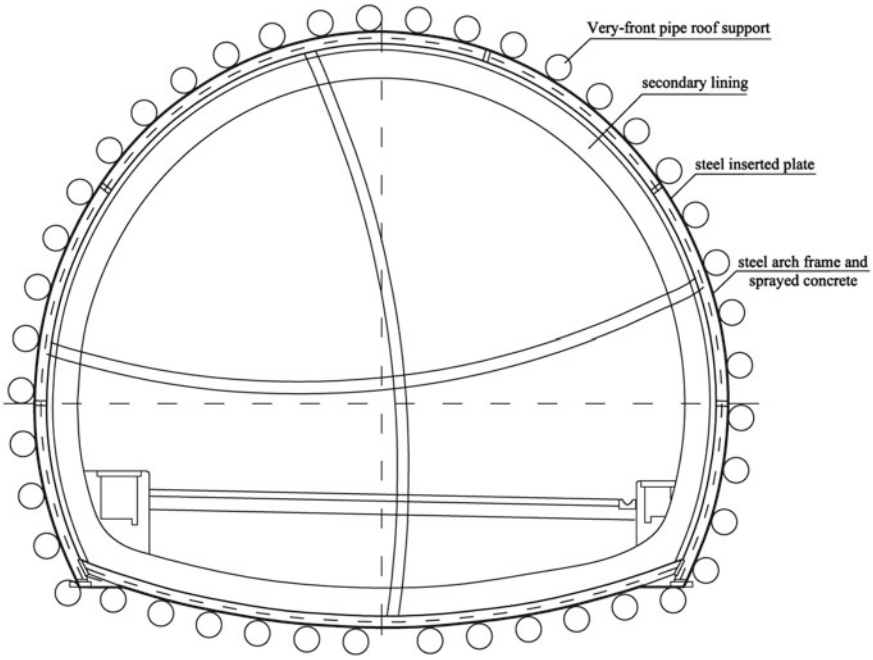


Fig. 2.41 Schematic diagram of surrounding steel inserted plate support structures specific to very front pipe roof support

section of a tunnel can be reinforced by using high-pressure jet grouting pile; the primary design parameters are listed as follows, as shown in Fig. 2.44.

(a) Triple tube high-pressure jet grouting pile method was used;
(b) Pile diameter: Φ800 mm; vertical interval: 1200 mm; horizontal interval 1200 mm; pile arrangement: plum blossom-shaped arrangement;
(c) Solidification agent: 42.5R composite Portland cement; and
(d) Area of reinforcement: 3 m each around the excavation contour line and the entire cross-section area of the tunnel face.

(2) Area of ground reinforcement
Pipelines below the road surface of highways are complex; executing ground reinforcement operations while circumventing nearby pipelines is challenging. Therefore, the recommended plan of improvement involves considering the temporary road closure and the removal or temporary closure of pipelines to comprehensively reinforce the top part of the tunnel. In total, 8141 m^2 of area was reinforced, as shown in Figs. 2.45 and 2.46. Principles underlying pipeline reconnection are as follows:

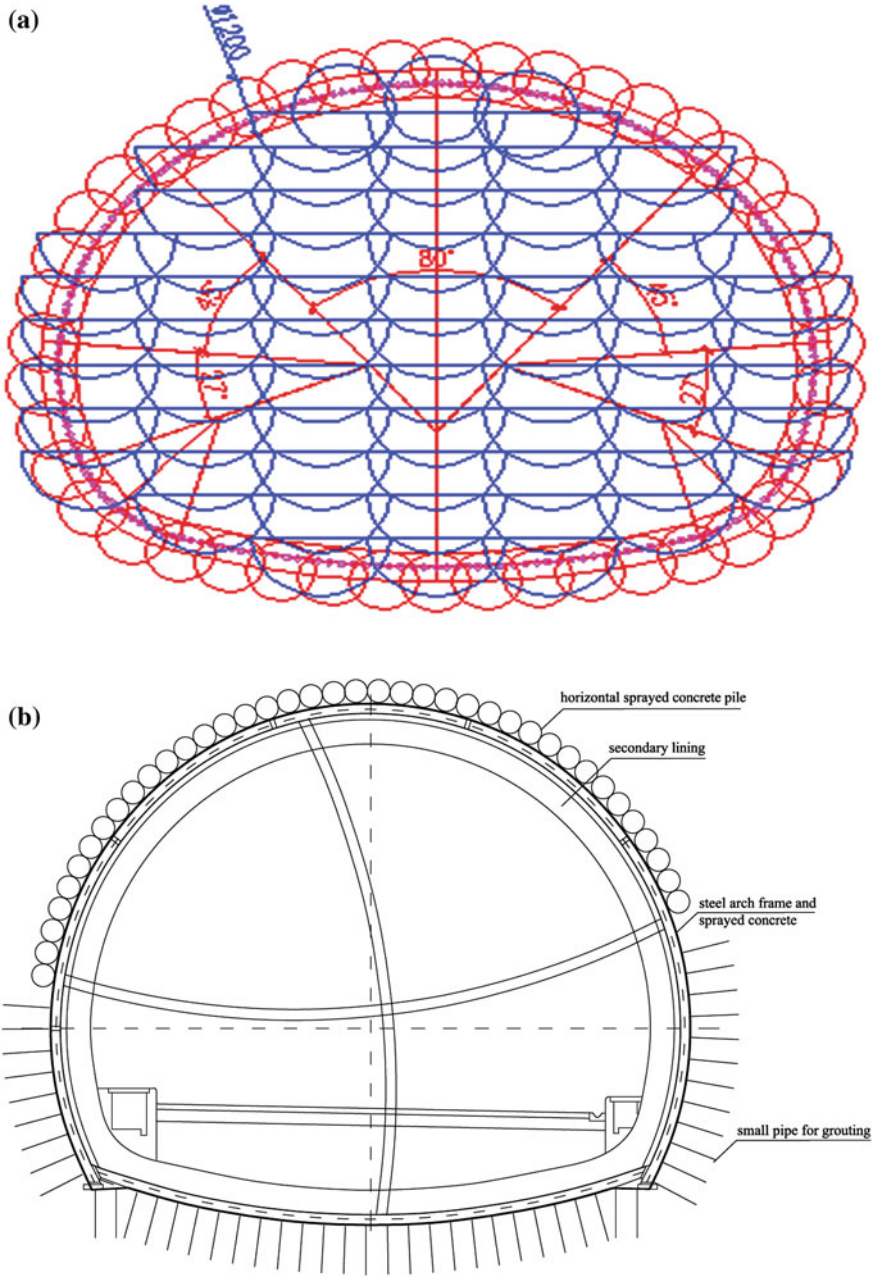


Fig. 2.42 Schematic diagram of very front support structure made of horizontal sprayed concrete pile

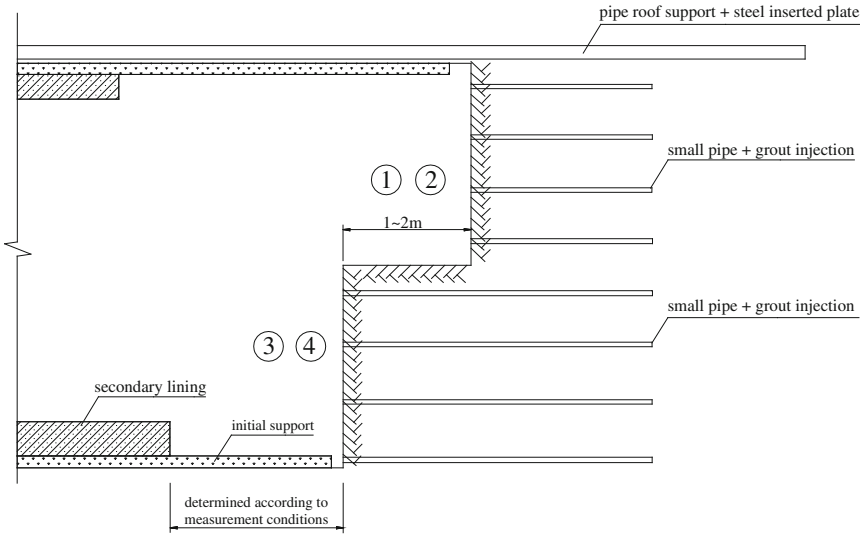


Fig. 2.43 Schematic diagram illustrating the longitudinal excavation of a tunnel

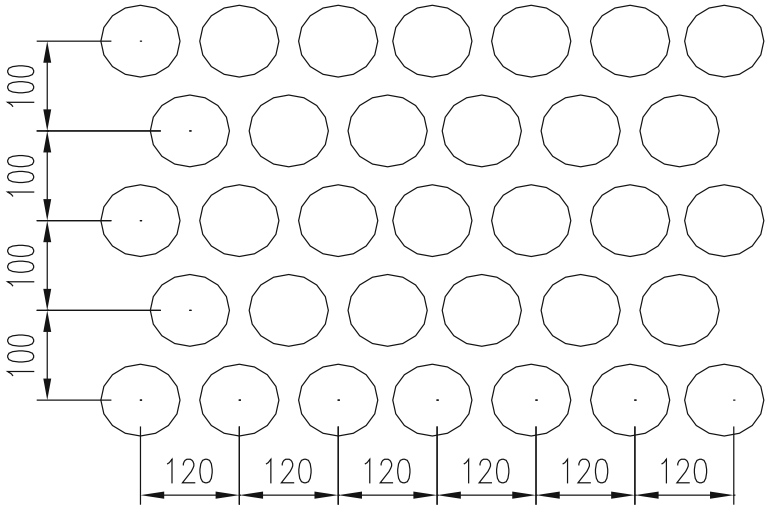


Fig. 2.44 High-pressure jet grouting pile arrangement

(a) Discontinue using the DN800 water supply pipe and protect it;
(b) Discontinue using the gas pipeline and protect it;
(c) Temporarily change the DN1000 water supply pipe to DN600 open pipeline, and then protect the original water supply pipe;
(d) Place soft pipeline inside the DN1000 waste discharge pipeline to strengthen discharge process and then protect the discharge pipeline.

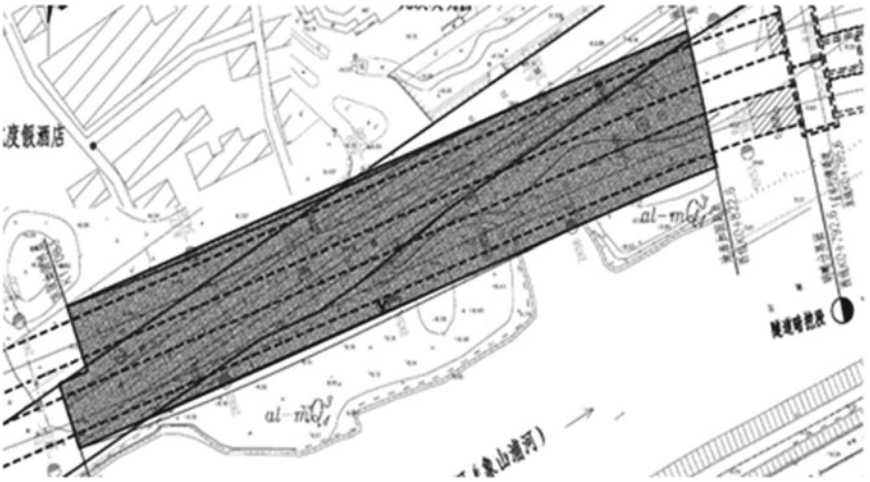


Fig. 2.45 Floor plan of high-pressure jet grouting pile

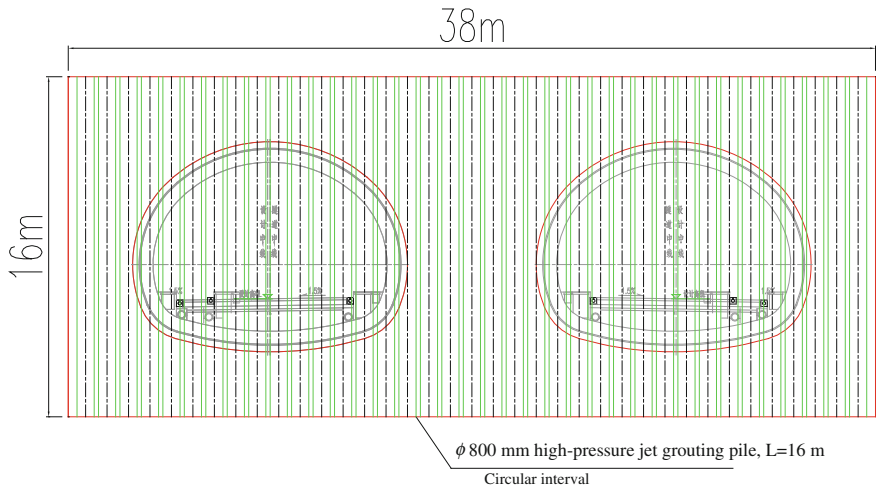


Fig. 2.46 Cross section arrangement of high-pressure jet grouting pile

Meanwhile, considering the safety of communication lines, power cables and original pipelines, no reinforcement was performed within 1 m of the two sides. Horizontal reinforcement grouting was applied on the blind spot of tunnel face, as shown in Fig. 2.47.

(3) Complete construction of 30 m-long pipe roof support at the tunnel entrance

Construction of lead pipe roof support within 30 m of the east and west-line tunnel entrance was completed. Thus, vertical jet grouting reinforcement

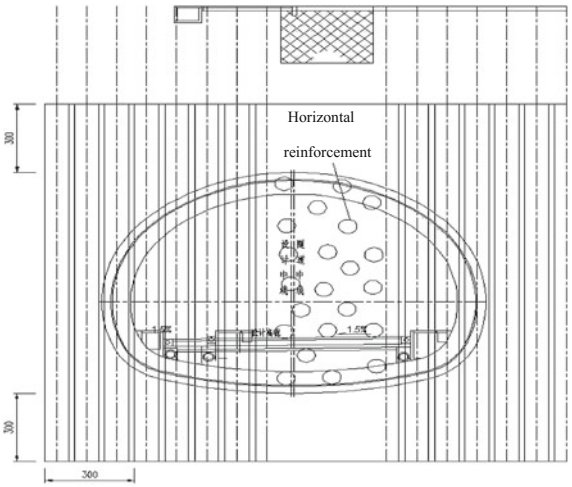


Fig. 2.47 Horizontal reinforcement grouting in the tunnel at the blind spot of high-pressure jet grouting pile reinforcement

could not be implemented on the ground 3 m below the arch base and within 30 m of the excavation contour line. Therefore, vertical reinforcement were performed on ground soil within 3 m of the top of the arch and on the two sides of the excavation contour line. The remaining portions were reinforced by using horizontal rotation spraying.

Horizontal jet grouting piles are installed at the tunnel face. The piles are 18 m long, and 600 mm in diameter, arranged in 1.0 m × 1.0 m plum blossom-shaped configuration, and connected one after another in a circular formation to form a circumference of 3 m, as shown in Fig. 2.48.

The cost of this implementation plan increased by approximately RMB26.08 million. The ground high-pressure jet grouting piles exhibited favorable reinforcement effects and required few cross-operations, thus substantially shortening the construction duration. However, the reinforcement operation considered only temporarily removing communication and power cables and thus could easily damage other pipelines during the construction process. Such operation still poses certain risks.

This implementation plan, in essence, involves using piles to reinforce soft soil and spraying concrete around the excavation contour line to form a pile +shell structure. The principle of mechanics behind this implementation plan is similar to the recommended plan (constructing surrounding steel inserted plate supports specific to lead pipe roof supports). Comparing both plans reveals that the implementation plan is expensive but more effective.

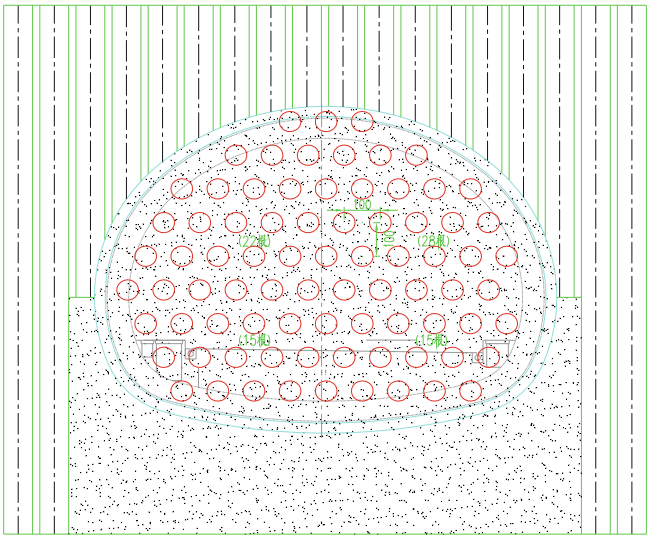


Fig. 2.48 Elevation view of high-pressure jet grouting pile reinforcement at the large pipe roof support section

2.4 Application Effectiveness of Deformation Compatibility Control Method in the Management of "Bump at Bridgehead" on Soft Soil Road Foundation

Long structures on soft soil road foundations are considered a plane strain problem that substantially influenced by the rheological properties of soft soil. Previous design considerations included soft soil consolidation and secondary consolidation, neglecting the comprehensive effects of soil and stone mixtures on road foundations. Consequently, the overcoming adverse effects of rheological properties of soft soil flow is difficult, which causes uneven subsidence on road subgrades at the head of the bridge, thereby resulting in the **development of bumps at bridgehead phenomenon** (hereafter referred to as bridgehead road bumps).

In the management of bridgehead road bumps on highway soft soil foundation, various types of pile foundations are feasible options to treat such foundation. However, mixed-in-place piles are superior to rigid piles as soil softness increases. According to **structure DCC improvement design methods**, attention must be paid to controlling the integrity and transition of stress–deformation state along the longitudinal direction in road foundation. In particular, the longitudinal transition length of the lower partition plate and pile is highly related to the changing elevation of bridge-head road foundation (e.g., lower partition plate, dust, and injected

grout; for foam concrete and EPS (Expanded Polystyrene), care should be exerted on their overall control and control of even distribution of vehicle load on structural layers). **Bridge-head road bumps can be managed** by controlling uneven subsidence of bridge-head road foundation within acceptable level.

2.4.1 Uneven Subsidence of Soft Soil Road Foundation

Road foundations on soft subgrade soil feature large pores, high compressibility, high moisture content, low permeability, low strength, strong rheological properties, structural formation, and high sensitivity. These characteristics render soft soil road foundations prone to uneven subsidence. The core problem of land subsidence is the inconsistency between the actual stress–deformation state of road foundation containing soft soil and rock fragments (Fig. 2.49a) and that of the design analysis model (Fig. 2.49b).

An ideal road foundation is a continuum model, whereas a road foundation composed of rock fragments is a discrete foundation. These two models differ primarily in that discrete bodies can withstand pressure but cannot bear tension and torque forces, whereas continuum bodies have the capacity to bear pressure, tension, and torque.

In engineering practice, vehicle load is a typical dynamic load (according to statistics for a harbor port, a vehicle can bear an overload exceeding 200 t) that creates a distinctive concave-shaped area on the bottom of the road foundation (as shown in Fig. 2.49a). This area is not an ideal purely pressure region (Fig. 2.49b). At this point, if the road foundation is still considered a continuous model with uniform load distribution as specified in existing regulations (Fig. 2.49b), then a great error will be generated.

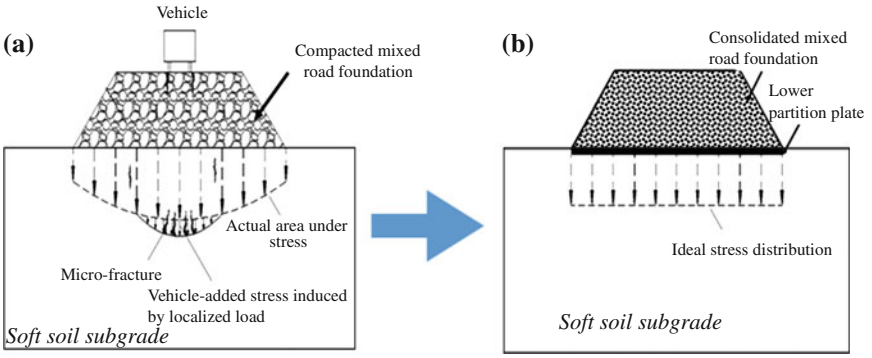


Fig. 2.49 Comparison of stress–deformation state of soft soil rock fragment road model and design model. **a** Stress model in practice. **b** Design analysis model

Currently, numerous measures are used to ensure the overall stress–deformation state of road foundations such as EPS, foam concrete, and lower partition plate. Particularly, EPS and foam concrete not only changed the overall stress–deformation state of road foundations but also altered the amount of load. The lower partition plate changed only the overall stress–deformation state of road foundations. The following engineering case is used as an example to first describe the effects of the overall stress–deformation state of road foundations and then conduct a quantitative study.

Construction of a narrow bridge on a multiple track west of National Highway 104 involved increasing the width of an old bridge. The height of the soil filled in the abutment was 2.4 m and the soil layer was 39.5 thick. The old bridge commenced operation in 1999, and its breadth was increased in 2009. The old bridge was maintained with the traditional upper transition slab method, and the broadened bridge was maintained with direct filling of rock fragments in the lower partition plate. The old bridge still continued to subsidize exceeding the amount the soft foundation subsided at the head of the broadened bridge. The total amount of subsidence was 11.23 cm. After seven years of operation, the new part of the broadened bridge measured a total subsidence of 4.75 cm, and no substantial uneven subsidence was observed, as shown in Fig. 2.50.

The aforementioned discussion indicates that principle of mechanics is required to extensively explore the reason causing uneven subsidence in soft road foundation. Only through this approach can effective management methods be identified. Through numerous attempts of mechanical experiment on stress–deformation state of soft soil road foundation, the following curve of the soft soil stratum engineering safety of Road No. 2 was obtained as shown in Fig. 2.51.

Based on rheological properties, Fig. 2.51 illustrates the safe boundary line of muddy soft soil under 50 kPa of normal stress. When soft soil deformation is within the boundary line, the structure is in a natural safe state, that is, the structure is in a state of compatible deformation. Conversely, when soft soil deformation is beyond the boundary line, the structure is in an unsafe state, which represents a state of



Fig. 2.50 Comparison of the old road with the added road following multiple track expansion on the west of a national highway

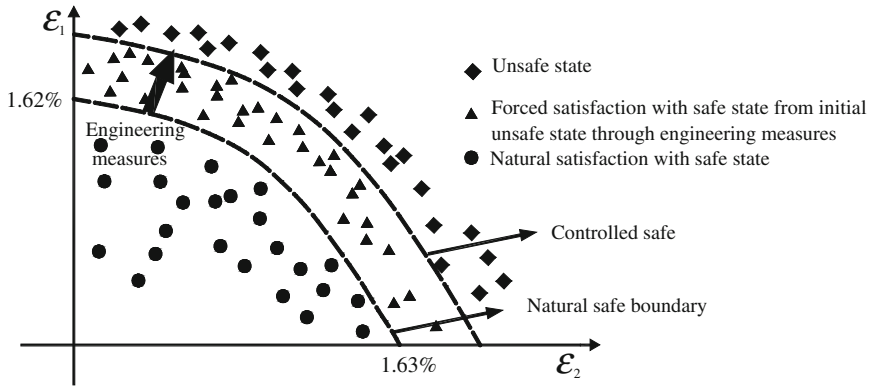


Fig. 2.51 Soft soil stratum engineering safety curve

incompatible deformation. However, engineering measures can be adopted to construct compulsory safety boundary line so that soft soil in unsafe state is forced to remain in a safe state. For example, grout injection, pile foundation, and lower partition plate can be used to increase the safety boundary line of soft soil, thereby making the entire structure deformation compatible and forcing it to be in a safe state.

2.4.2 Comparison Test and Calculation Analysis of Integrity and Friability of Bridge-Head Soft Soil Road Foundation

Drilling was performed to acquire core samples from different road foundations, specifically Highway No. 1 with friable road foundation and Highway No. 2 with intact road foundation. Highway No. 1 and No. 2 are both in soft soil region and not far apart from each other.

Vertical sampling was conducted on soft soil road foundation by acquiring one soil sample from an average depth of 1 m. Comparison of the foundation structure of roads No. 1 and No. 2 is presented in Table 2.3.

Comparison of Fig. 2.52a, b shows that Highway No. 2 is built on a calcareous soil foundation acting as an intact structure which homogenizes the stress distribution of soft soil foundation, whereby uneven subsidence of road foundations can be controlled. Conversely, Highway No. 1 is built on rock fragment foundation and is considered a friable structure. Under vehicle dynamic load, this type of foundation easily causes stress concentration, gradually resulting in uneven settlement.

Traditional soft soil foundation stress analysis generally considers rock fragments as a uniform continuum body. Therefore, vehicle load equivalent to a static load of approximately 0.5 m of covered soil is evenly distributed on soft soil

Table 2.3 Comparison of the foundation structure of roads No. 1 and No. 2

	Hole No.	Road surface	Cement stabilized crushed stone (CSCS) layer	Road foundation
Road No. 1	HZK2	0–0.15 m asphalt concrete	0.15–0.55 m CSCS	0.55–2.5 m stonewall (earth–stone mixture)
	HZK3	0–0.15 m asphalt concrete	0.15–0.63 m CSCS	0.63–2.1 m stonewall (earth–stone mixture)
	HZK4	0–0.15 m asphalt concrete	0.15–0.75 m CSCS	0.75–2.3 m stonewall (earth–stone mixture)
Road No. 2	ZK2	0–0.15 m asphalt concrete	0.15–0.52 m CSCS	0.52–2.2 m calcareous soil
	ZK3	0–0.15 m asphalt concrete	0.15–0.52 m CSCS	0.52–2.0 m calcareous soil
	ZK4	0–0.15 m asphalt concrete	0.15–0.53 m CSCS	0.52–2.1 m calcareous soil
Comparison		Basically identical		Considerable difference

foundation. However, this is not the case in practice (Fig. 2.53). The section below presents a specific calculation that quantitatively analyzes the load-bearing of a soft soil foundation in realistic engineering conditions.

According to Technical Standard of Highway Engineering (JTG B01-2014), typical vehicle parameter is a vehicle weight of 550 kN (approximately 55 t); four tires in the middle and four rear tires each touch the ground at a breadth and length of 0.6 m × 0.2 m, and two front tires touch the ground at a breadth and length of 0.3 m × 0.2 m. The outer dimension of the vehicle is 15 m × 2.5 m.

The density of rock fragment foundation is 2000 kg/m^3; the density of calcareous soil foundation is 1730 kg/m^3. Initial flow stress of soft soil foundation is 26 MPa.

Figure 2.54 and 2.55 illustrates the stress analysis of the intersection between the soft soil in the soft soil road foundation and the road foundation when the road foundation is filled up to a height of 1.5 m and 1.2 m, respectively.

Therefore, the road foundation on Highway No. 2 has low elevation and weighs approximately 30% lighter than that on Highway No. 1. Overall, the road foundation is light weight and is intact, which effectively avoids the barriers to using Terzaghi's Principle and the unfavorable effects of concentrated vehicle dynamic load. Therefore, the foundation conforms to the design stress model for a road foundation, which is the fundamental reason for the absence of uneven subsidence on the road foundation.



Fig. 2.52 Comparison of soft soil core samples of No. 1 and No. 2 road foundations. **a** Soft soil core samples of Road No. 1 (friable foundation). **b** Soft soil core samples of Road No. 2 (intact foundation)

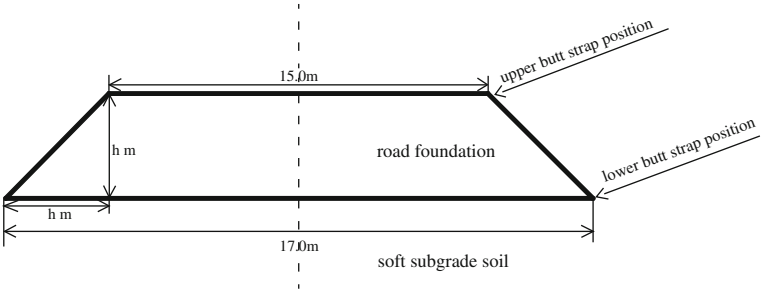


Fig. 2.53 Stress analysis model of soft soil road foundation

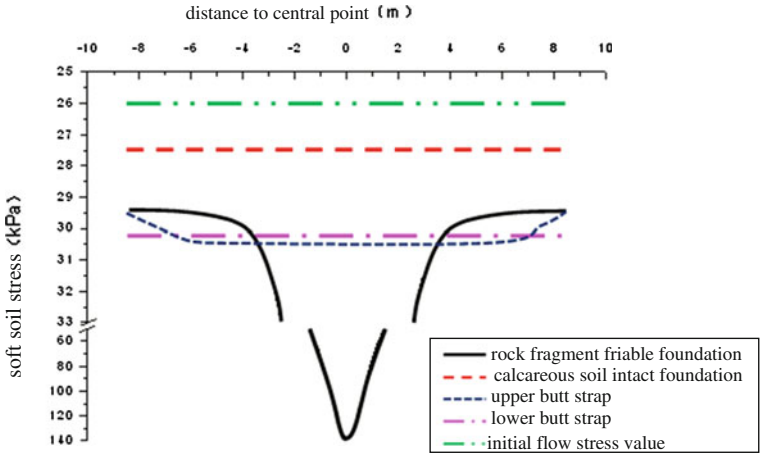


Fig. 2.54 Stress analysis of the intersection between the soft soil in the soft soil road foundation and the road foundation when the road foundation is filled up to a height of 1.5 m

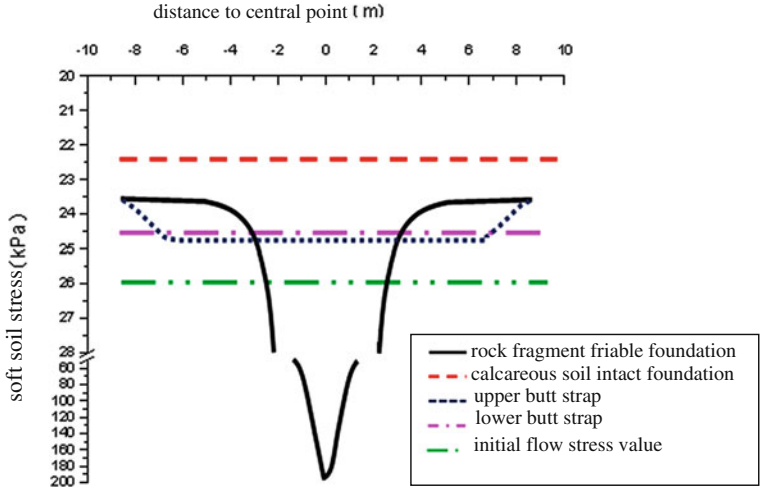


Fig. 2.55 Stress analysis of the intersection between the soft soil in the soft soil road foundation and the road foundation when the road foundation is filled up to a height of 1.2 m

According to the aforementioned calculation, evenly distributing vehicle load and neglecting the concentration effect of vehicle dynamic load essentially influences the calculation result. This analysis result is consistent with the uneven settlement observed from over 30 years of highway construction and operations.

Comparison and calculation analysis of the integrity and friability of a soft soil road foundation at the head of a bridge show that intact road foundation

exhibits superior stress–deformation characteristics compared with that of friable road foundation. Hence, the integrity of stress–deformation state of a road foundation must be controlled during the design and construction process to ensure that the state meets regulatory requirements.

2.4.3 Comparison of Soft Soil Foundation Strength and Rheological Properties in Tests

(1) **Comparative Analysis of the Flow Property of Highway Roads No. 1 and No. 2 Soft Soil Foundation**

During sample preparation, the soft soil samples obtained from Highway Roads No. 1 and No. 2 were kept undisturbed to ensure that the mechanical behavior of laboratory soil samples was consistent with that in situ, as shown in Fig. 2.56.

A total of 96 specimens retrieved from Road No. 1 were usable, and 52 specimens from Road No. 2 were usable, yielding 148 usable specimens. Each specimen was subjected to a minimum loading time of 144 h and maximum loading time of 172 h. Two types of loading (25, 50, 100, and 200 kPa as shown in Fig. 2.57 or 50, 100, 200, and 400 kPa) were used in accordance with the soil properties. At the beginning of the test, data were recorded every hour, and then every 4 h at the later stage of the test.

Figure 2.57 shows that at the initial stage, soft soil subsidence increased significantly with time, and the increasing trend gradually diminished, approaching a stable state. Comparison of subsidence at stress levels of 25, 50, 100, and 200 kPa reveals that when the stress level is 25 kPa, the rheological effect on soft soil subsidence is negligible. When the stress levels are 50, 100, and 200 kPa, the rheological effects on soft soil subsidence are substantial. Based on these results, the concept of initial flow stress is proposed. The definition of this concept is that when stress level is lower than the initial flow stress, the rheological effect is small; when the stress level is higher than the initial flow stress, neglecting the rheological effect on soft soil subsidence can exert tremendous influence on the result.

To objectively compare the mechanical properties of Roads No. 2 and No. 1 soft soil foundations, the effect of the peat soil layer was removed from the observation results from the soft soil foundation of Road No. 2, and mean loading values were obtained. Meanwhile, because the soft soil layer of Road No. 1 is thinner than that of Road No. 2, soft soil samples within a depth of 6.5 m in both foundations were obtained for comparison. The result of comparison is shown in Table 2.4.

Table 2.4 indicates that the engineering characteristics of Roads No. 1 and No. 2 differed by within 4% on overall. The effect of such minimal difference in highway engineering can be neglected.

When the effect of peat soil is eliminated, the final subsidence of soft soil foundation on Road No. 2 was slightly smaller than that on Road No. 1. However, the subsidence after construction due to the rheological properties in the soft soil on



Fig. 2.56 Samples used in indoor flow testing. **a** Hole No. 1. **b** Hole No. 2

Road No. 2 is larger than that in soft soil on Road No. 1. In reality, the road foundation on Road No. 2 exhibits uneven subsidence that is smaller than that on Road No. 1. Therefore, **examination of uneven subsidence of soft soil road foundation must involve not only the mechanical properties of the soils, but also the stress–deformation model of the foundations**.

(2) **Comparative Analysis of Strength and Flow Properties of Soft Soil Foundations in Tests**

In mechanics, initial flow stress value and strength value are two completely different concepts. Strength refers to the maximum stress a material can sustain

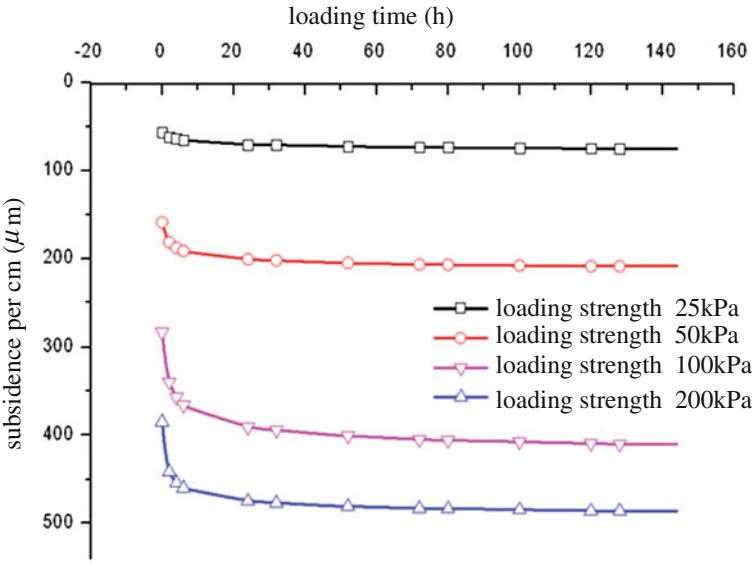


Fig. 2.57 Flow curve of Road No. 1 soft soil (Sample No. 5 from Hole No. 2, soil depth of 5 m)

Table 2.4 Comparison of mechanical properties of soft soil foundation on Roads No. 1 and No. 2

	Flow subsidence value (μm/cm)	Initial flow stress (KPa)
Road No. 1	11.63	26
Road No. 2	12.01	23

during the loading process before reaching failure. Initial flow stress refers the minimum stress at which a material demonstrates significant creep under long-term load. In actual applications, the initial flow stress of a material is equivalent to its strength value; therefore, these two concepts are often used interchangeably, specifically for engineering materials with greater rigidity such as hard rocks. Soft soil and rocks differ in that the initial flow stress and strength of soft soil are considerably different. Figure 2.58 presents an intuitive comparison of initial flow stress and strength of soft soil. According to this figure, the soft soil initial flow stress is approximately 20% of the strength of the soft soil. Hence, for soft soil foundations, the initial flow stress of undisturbed soft soil foundation is far smaller than its strength. If strength value is applied in calculation analysis, a large error will be generated. Particularly, when soft soil foundation is exposed to maximum stress for long period, the creep becomes increasingly evident, suggesting that flow value, rather than strength, should be adopted in actual calculation analyses.

In summary, initial flow stress value and strength value are two distinct concepts and therefore clear distinctions between these two concepts must be made when the stable equilibrium of engineering structures is calculated.

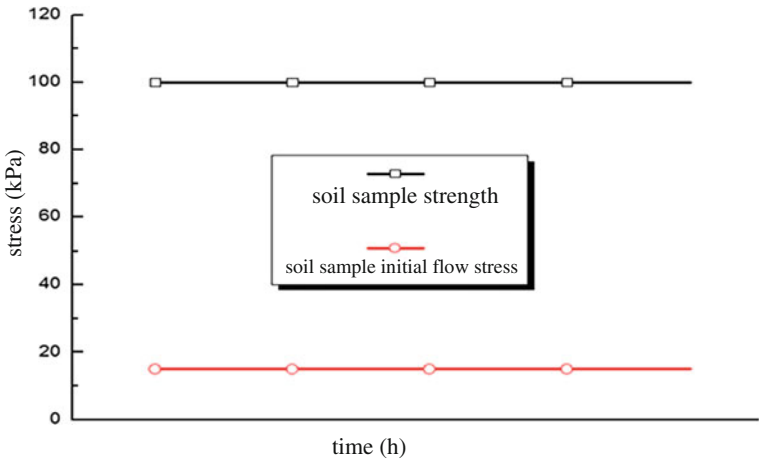


Fig. 2.58 Difference between the strength and initial flow stress of muddy soil

2.4.4 Basic Law and Design Method for Soft Soil Foundation

A summary of the soft soil road foundation conditions examined above is provided in Table 2.5.

Structural comparison of Roads No. 1 and No. 2 as shown in Table 2.5 and Fig. 2.59 reveals that both roads differ substantially regarding their composition in foundation. Road No. 1 is built on rock fragment foundation, exhibiting friable foundation that negatively influences the load bearing capacity of soft soil foundation. By contrast, Road No. 2 is built on calcareous soil, exhibiting higher integrity than that of Road No. 1. Concentrated load is evenly distributed, controlling deformation in soft soil foundation.

Nevertheless, management of uneven subsidence in soft soil road foundation must consider not only the characteristic of the foundation but also the stress–

Table 2.5 Structural comparison of Roads No. 1 and No. 2

Region	Road No. 1	Road No. 2	Result
Indicator			
Road surface	Approx. 0.15 m asphalt concrete	Approx. 0.15 m asphalt concrete	Basically identical
CSCS layer	0.4–0.6 m CSCS	Approx. 0.4 m CSCS	Basically identical
Road foundation	1.5–2.0 m rock segment (friable road foundation)	1.5–1.7 m calcareous soil (intact road foundation)	Significant difference
Soft soil flow characteristics	11.63 μm/cm flow subsidence	12.01 μm/cm flow subsidence	Basically identical



Fig. 2.59 Comparison of soft soil road foundation on Roads No. 1 and No. 2. **a** Condition of intact foundation on Road No. 2. **b** Condition of friable foundation on Road No. 1

deformation model of the foundation. The two key points of subsidence management are as follows:

(1) Control the integrity of the stress–deformation state of the road foundation so that concentrated load is evenly distributed to reduce peak load value and avoid the load from exceeding the initial flow stress of soft soil foundation, which would otherwise cause uneven subsidence.
(2) Stable equilibrium between the weight of the road foundation and load bearing capacity of soft soil foundation involves the road foundation weight and initial flow stress of the soft soil foundation. Stable equilibrium can be achieved using the following two approaches: (a) Increasing strength of soft soil foundation, that is, reducing its creep deformation; and (b) reducing the top load on soft soil foundation so that the foundation stress is lower than the initial flow stress of the soft soil foundation, thereby satisfying the mechanics control goal, that is, the top load (including load evenly distributed in the road foundation and localized traffic dynamic load) is smaller than the load bearing capacity of soft soil foundation.

According to the aforementioned study results, specific measures for managing the uneven subsidence of soft soil road foundations (e.g., road bumps) can be implemented in two steps:

(1) Controlling the integrity of stress–deformation state of road foundation: The integrity of stress–deformation state of road foundation can be controlled by using EPS, foam concrete, or calcareous road foundations; installing lower partition plate; and adding frames to pile foundation. Thus, subsidence due to friability of road foundation can be reduced.
(2) Soft soil road foundation design method: (a) Conduct creep tests on soft soil to verify the initial flow stress values of such foundations; (b) calculate the stress value of the bottom part of the soft soil foundation; and (c) compare and design stress value, in which, if the initial flow stress of the soft soil foundation is larger than the calculated stress value of the bottom part of the soft soil foundation, then uneven subsidence of soft soil road foundation can be controlled. If the initial flow stress of the soft soil foundation is smaller than the calculated stress value of the bottom part of the soft soil foundation, then engineering measures must be adopted, such as low weight road foundation or adding frames to pile foundation, in order to control uneven subsidence of soft soil road foundation.

2.4.5 Introduction to Successful Management of Soft Soil Road Foundations

Problems associated with uneven subsidence of soft soil road foundation can be solved by controlling the stress of such foundation within its initial flow stress according to the characteristics of the foundation. Alternatively, corresponding engineering measures can be adopted.

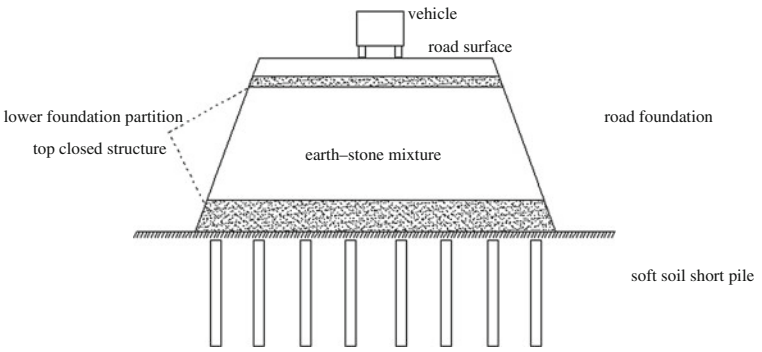


Fig. 2.60 Addition of lower partition plate + short pile

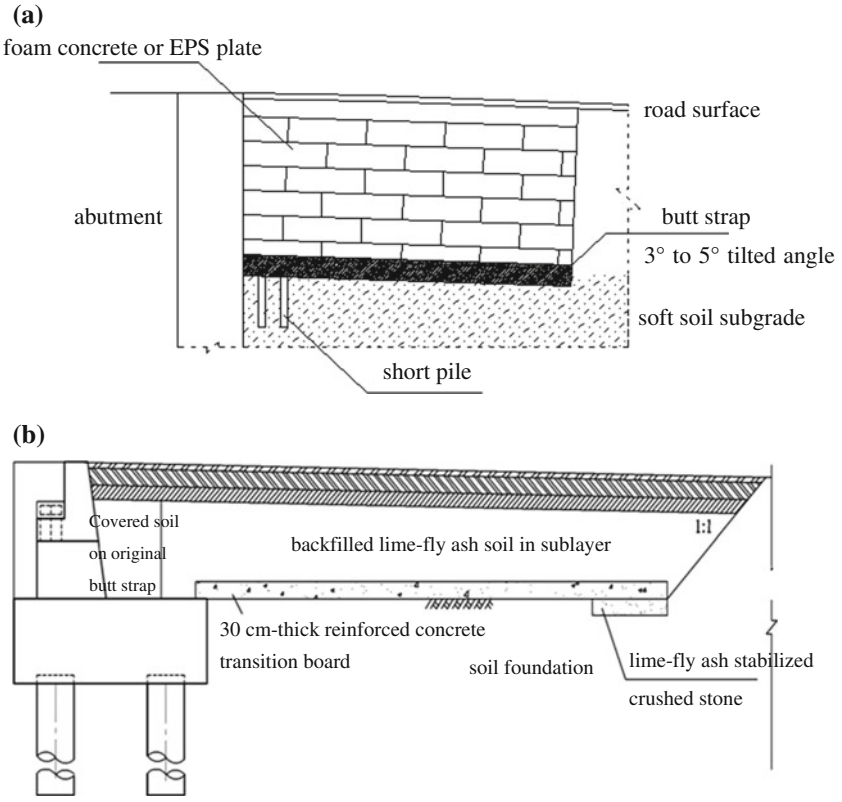


Fig. 2.61 Foam reinforced concrete, EPS board + deep layer butt strap

In fact, bumps at bridge-heads can be effectively managed simply by determining the integrity of the stress–deformation state of the soft soil road foundation, the law of flow in soft soil foundations, and corresponding response measures. Figures 2.60 and 2.61 **illustrate the successful measures used to manage soft soil road foundations. These measures are difficult to understand if their underlying mechanisms remain obscure, but if they are understood, these measures become crystal clear**.

In the management of bridge-head road bumps on highway soft soil foundation, various types of pile foundations are feasible options to treat such foundation.

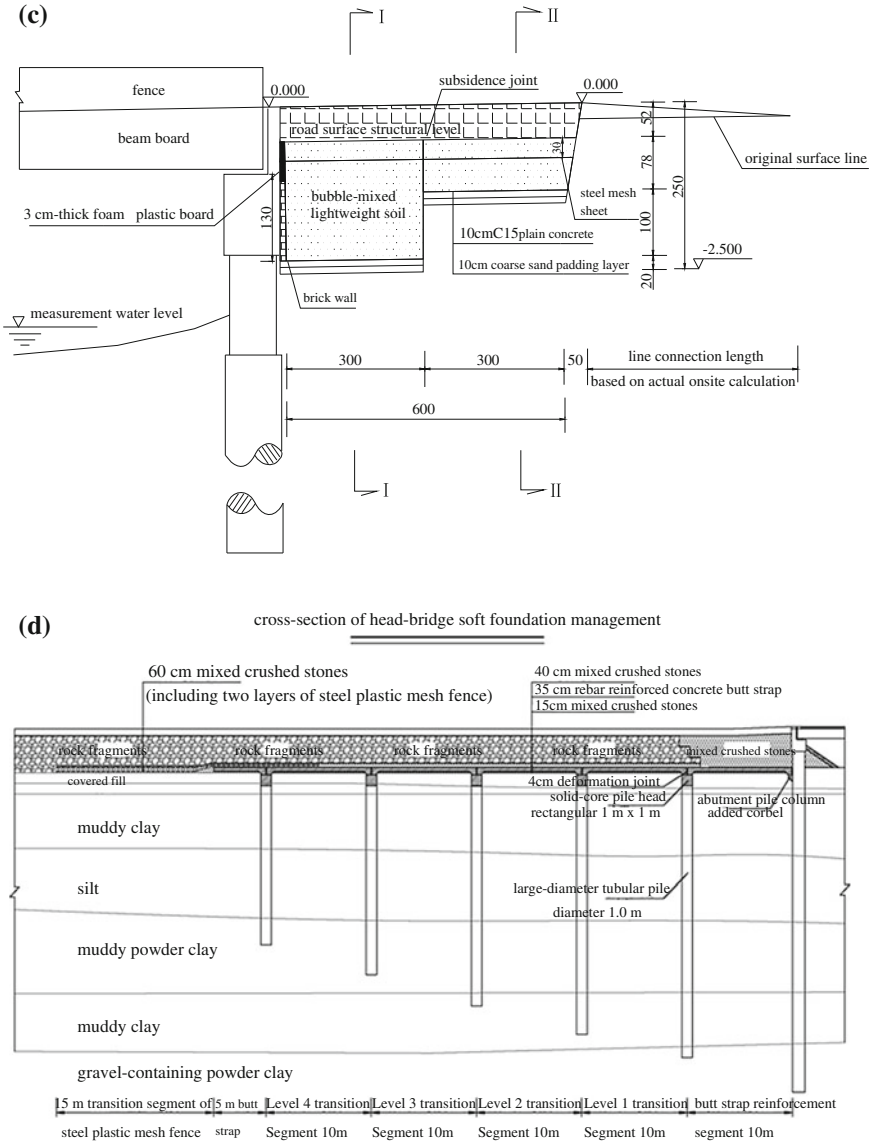


Fig. 2.61 (continued)

The key lies in controlling the integrity and longitudinal transition of stress–deformation states in road foundations (e.g., lower partition plate, lime clay, and injected grout; for foam concrete and EPS, care should be taken regarding their overall control and control of even distribution of vehicle load in structural layer).

http://www.springer.com/978-981-10-1892-3

Deformation Compatibility Control for Engineering Structures
Methods and Applications
Zhu, H.; Zhou, Z.; Chen, M.; Deng, J.
2017, XII, 116 p. 84 illus., 45 illus. in color., Hardcover
ISBN: 978-981-10-1892-3